

<https://doi.org/10.33472/AFJBS.6.6.2024.6275-6313>



African Journal of Biological Sciences

Journal homepage: <http://www.afjbs.com>



Research Paper

Open Access

Synthesis, Characterization, Docking Studies and Invitro Response of Novel 1, 3-Indanedione Derivatives Against Drug Resistant Tuberculosis

Nitin Londhe¹, Karthickeyan Krishnan^{2*}

¹Research Scholar, School of Pharmaceutical Sciences, Vel's Institute of Science, Technology and Advanced Studies (VISTAS), Pallavaram, Chennai, Tamil Nadu, 600117, India.

²Professor & Head, Department of Pharmacy Practice, School of Pharmaceutical Sciences, Vel's Institute of Science, Technology and Advanced Studies (VISTAS), Pallavaram, Chennai, Tamil Nadu, 600117, India.

Corresponding Email: ^{2*}karthickeyanpharmacy@gmail.com

Article Info

Volume 6, Issue 6, June 2024

Received: 23 April 2024

Accepted: 31 May 2024

Published: 26 June 2024

[doi: 10.33472/AFJBS.6.6.2024.6275-6313](https://doi.org/10.33472/AFJBS.6.6.2024.6275-6313)

ABSTRACT:

1,3-Indanedione pharmacophore become a promising nucleus for researcher because possesses wide ranges of biological activities. Cyclic diketones 1,3-indanedione derivatives have synthesized via Knoevenagel condensation, by condensing different aromatic aldehydes with 2-(aryl methylene)-(1*H*)-indane-1,3-(2*H*)-dione **1** in the presence of alcoholic-piperidine as solvent leading to the formation of different C₂ substituted 2-benzylidene-1*H*-indene-1,3(2*H*)-diones. On reacting diethyl phthalate (DEP) with ethyl acetate using sodium metal catalyst in alcoholic solution and later acid neutralization affords 1,3-Indanedione **1**. The newly designed title compounds have been characterized by FTIR, ¹NMR, mass spectral data. The in-vitro MABA carried out for their antitubercular activities against *Mycobacterium tuberculosis* H37Rv strain.

MIC values found 4.5 μM to 167 μM, the results shown compound 1, 10, 11, 12, 15 demonstrated exceptional potential to inhibit *M. tuberculosis* compared to standard Isoniazid whereas compounds 2, 3, 4, 5, 6, 7, 8 and 14 showed moderate activity and 7, 8 showed less activity as compared to standard INH. Molecular docking studies against 6SQ5 enzyme with compounds 11, 6, 9 and 1 exhibited the highest binding energy of -9.9, 9.6, 9.5, and -9.2 kcal/mol, respectively.

PASS prediction identifies various biological functions and ADMET lab 2.0 program to compute the drug physicochemical as well as medicinal properties of various substituted 2-(aryl methylene)-(1*H*)-indane-1,3-(2*H*)-diones derivatives.

Keywords: Indane dione, Knoevenagel condensation, ADMET lab 2.0, Pass prediction Antitubercular activity.

© 2024 Nitin Londhe, This is an open access article under the CC BY license (<https://creativecommons.org/licenses/by/4.0/>), which permits unrestricted use, distribution, and reproduction in any medium, provided you give appropriate credit to the original author(s) and the source, provide a link to the Creative Commons license, and indicate if changes were made

1. Introduction

Cyclic diketones Indane-1, 3-dione derivatives represent a unique group of compounds and researcher found this nucleus possessing wide range of applications in variety of diseases [1, 2]. Indane-1, 3-dione derivatives substituted at 2 position or phenyl substituted halogens or electron donating or accepting groups forms compounds that represents most biologically active classes, shown wide spectrum of activities. Various substituted indane-1,3-dione [3-5] derivatives are associated with diverse pharmacological activities such as, anthelmintic [6] anticoagulant [7], analgesic [8], anti-inflammatory [9,10], anticancer [11,12], antibacterial, antifungal [13,14], tomato damping –off disease [15] psychopharmacological activities [16]. Similarly Other biological activities includes anti- β amyloid aggregation, cholinesterase inhibition, neuroprotection properties against Alzheimer's disease [17], hGlyT1 inhibition [18], embryotoxic and teratogenic activities [19], anti-allergic activity [20] and cervical cancer antitumor activity[21].

Cyclic diketone indane-1,3-dione derivatives also shown there potential to inhibit neutrophil elastase involved in chronic obstructive pulmonary disease (COPD) and various lung tissue derangements, such as cystic fibrosis[22]. Studies on the medicinal chemistry of indane-1,3-dione have been intermittent.

Structurally cognate nucleus Indanone used in the designing of most of the biologically active compounds [23–25]. For the design of many different biologically active molecules Indane-1, 3 Dione have potential interest extensively studied as a synthetic intermediate [26].

Indane-1, 3-dione possesses an active methylene group, making this electron acceptor an excellent candidate for its association with electron donors by means of Knoevenagel reactions, presenting an interesting feature [27].

Knoevenagel reaction, which involves the condensation of compounds possessing active methylene groups with aldehydes or ketones to form α , β -unsaturated carbonyl compounds, is a well-known and valuable synthetic strategy. Indane-1, 3-dione, with its active methylene group, is indeed a suitable substrate for this reaction [27].

The active methylene group of indan-1, 3-dione provides a site for nucleophilic attack on the carbonyl carbon of aldehydes or ketones, resulting in the formation of a carbon-carbon double bond. This reaction is typically catalyzed by a base, such as piperidine or a secondary amine, which facilitates the deprotonation of the active methylene group, generating an enolate intermediate. Subsequent nucleophilic addition to the electrophilic carbonyl group of the aldehyde or ketone, followed by dehydration, affords the desired α , β -unsaturated carbonyl compound [29].

Mycobacterium tuberculosis, the etiological agent of tuberculosis (TB), remains a significant global health threat, causing immense morbidity and mortality worldwide. Despite concerted efforts to control the spread of TB, challenges persist due to the organism's unique biology, evolving drug resistance, and complex interactions with the host immune system. By synthesizing current knowledge and emerging research findings, this article aims to contribute to the collective understanding of M. tuberculosis and facilitate the development of more effective interventions to combat this ancient scourge [30-36].

In search of improved antitubercular drugs which overcome resistance to treatment , we represent herein , the synthesis of aryl chalcones namely 2-[(aryl)methylidene]-1*H*-indene-1,3(2*H*)-dione derivatives (1-15) by treating 1*H*-indene-1,3(2*H*)-dione with various substituted aromatic aldehydes utilizing alcoholic base catalyst piperidine by Knoevenagel condensation reaction. As per previously reported procedures, the initial starting material 1*H*-indene-1,3(2*H*)-dione synthesized as represented in Figure 1, Scheme I[37].

The 2-substituted aryl 1*H*-indene-1, 3(2*H*)-dione derivatives 1-15 synthesized as per Figure 2,3; Scheme II & III and confirmed by spectral data found in IR, ¹H NMR ,Mass spectrometry and elemental analysis.

All the compounds screened for in-vitro antitubercular activity against Standard strain M. tuberculosis, H37RV along with molecular docking studies against enoyl-acyl carrier protein reductase (InhA) enzyme.

2. Materials And Methods

Chemicals & Apparatus

All research chemicals were purchased from Merck or Cosmo Chem Pvt. Ltd. and used as such for the reactions. Solvents except LR grade were dried and purified according to the literature whereas necessary. The glasswares used in the reactions are made of borosil. All the glasswares were cleaned by using chromic acid and acetone before use. Open capillary apparatus were employed to determine melting points and found uncorrected.

List of instruments

Melting points of all compounds were determined in melting point apparatus. TLC was performed on microscopic slides (2×7.5 cms) coated with silica-gel-G and pre-coated silica gel strip. Solvent system (or) mobile phase was used with various ratios of n-Hexane: Ethyl acetate (4:1), Benzene: Methanol (4:1). Coloured spots travelled were visualized by exposure to UV light and iodine vapour. Mass spectra were recorded on ESI-MS Mass spectrometer at Cryogen MASS services, Mumbai. ¹HNMR spectra were obtained in DMSO on Bruker Advance-II 400 MHz instrument and chemical shift were measured as parts per million downfield from tetramethyl silane (TMS) as internal standard at Cryogen NMR services, Mumbai. Synthesis of novel series is shown in Scheme II & III.

Synthesis & Characterization

1. General procedure for the preparation of Starting Materials (indane-1,3-dione):

Scheme-1

Synthesis of indane-1, 3-dione [38-39] (I)

1. Diethyl phthalate (10.5 ml, 0.0563 mol) 1 and sodium wire (0.25 g), were heated on a steam bath which was taken in the two necked round bottom flask.
2. A mixture of dry ethyl acetate (1.36 ml, 0.139 mol) and absolute ethanol (2.5 ml) were added for a period of 90 min through the dropping funnel.
3. The mixture was refluxed for 6 h, and cooled. 50 ml of diethyl ether was added and mixed well.
4. The formed sodium salt was filtered, washed with ethyl acetate.
5. The residue was dissolved in hot water and the reaction mixture was cooled to 70°C.
6. Sulfuric acid (100 ml, 3 parts of acid to 1 part of water) was added to the mixture and further cooled to 15°C in ice bath.
7. The formed indane-1, 3-dione 2 was collected, washed with water and dried at 100°C.
8. The product was recrystallized from dioxane–benzene mixture by addition of light petroleum ether.

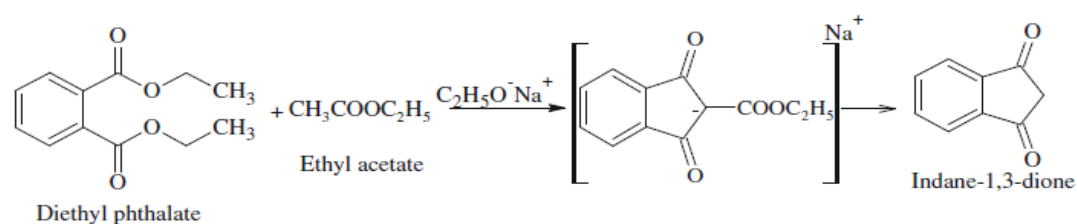
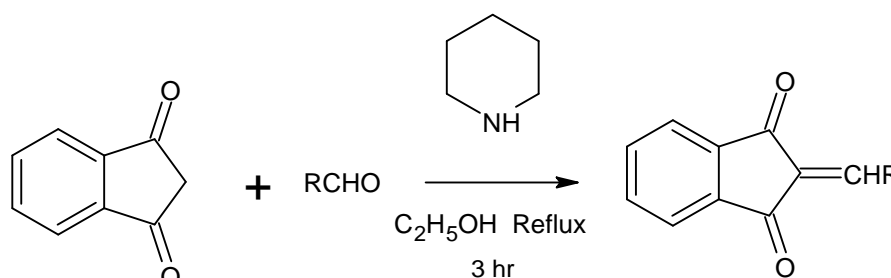


Figure 2, Scheme I- General design strategy of indane-1, 3-Dione

Scheme -2**General procedure for the preparation of 2-(aryl methylene)-(1*H*)-indane-1, 3-(2*H*)-diones, Knoevenagel condensation [40-41] (1-8)**

1. To an ethanolic solution of indane-1, 3-dione (14.6gm~0.1 mole) **2** were added different distilled aromatic aldehydes (12.6gm~0.1 mole) **3** followed by a drop of piperidine.
2. The mixture was refluxed for 3 hr.
3. The resultant reaction mixture was concentrated to half of its volume and poured onto crushed ice.
4. The solid that separated was filtered using vacuum pump and washed repeatedly with ice-cold aqueous ethanol.
5. Then it was recrystallized from ethanol.

Figure 3; Scheme II-Design strategy of 2-(aryl methylene)-(1*H*)-indane-1, 3-(2*H*)-diones

Compound Number	R
1	2-F,4-Cl C ₆ H ₃
2	2-Br,5-F C ₆ H ₃
3	3-NO ₂ C ₆ H ₄
4	3-Cl C ₆ H ₄
5	2,6(OCH ₃) ₂ C ₆ H ₃
6	4-(CH ₃) ₃ C ₆ H ₄
7	C ₆ H ₅
8	3-OH,4(OCH ₃)C ₆ H ₃

Scheme -3**General procedure for the preparation of 4-halogen substituted 2 aryl Indane-1, 3-dione (9-17)**

4-halogen substituted 2 aryl Indane-1, 3-dione (**9-15**) series synthesized using 4-substituted aromatic aldehydes on reacting with indane-1, 3-Dione. (Scheme III). To an ethanolic solution of indane-1, 3-dione (0.1 mole) were added different distilled 4-halogen substituted aromatic aldehydes (0.1 mole) followed by a drop of piperidine. The mixture was refluxed for 3 hr. The resultant reaction mixture was concentrated to half of its volume and poured onto crushed ice. The solid that separated was filtered using vacuum pump and washed repeatedly with ice- cold aqueous ethanol. Then it was recrystallized from ethanol [42].

Compound Number	R
9	2-OH,4-F C ₆ H ₃
10	3-OH C ₆ H ₄
11	4(3FCH ₃) C ₆ H ₄
12	4(OCH ₃ -CH ₂) C ₆ H ₄
13	(3,4 Dichloro) C ₆ H ₃
14	(3,5 Dichloro) C ₆ H ₃

15	$4(\text{CO-OCH}_3) \text{C}_6\text{H}_4$
----	---

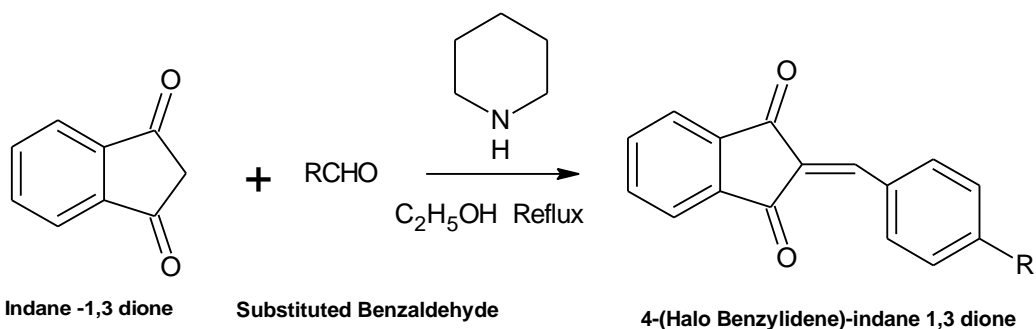


Figure 4; Scheme III- Design strategy of 4-halogen substituted 2 aryl Indane-1, 3-dione

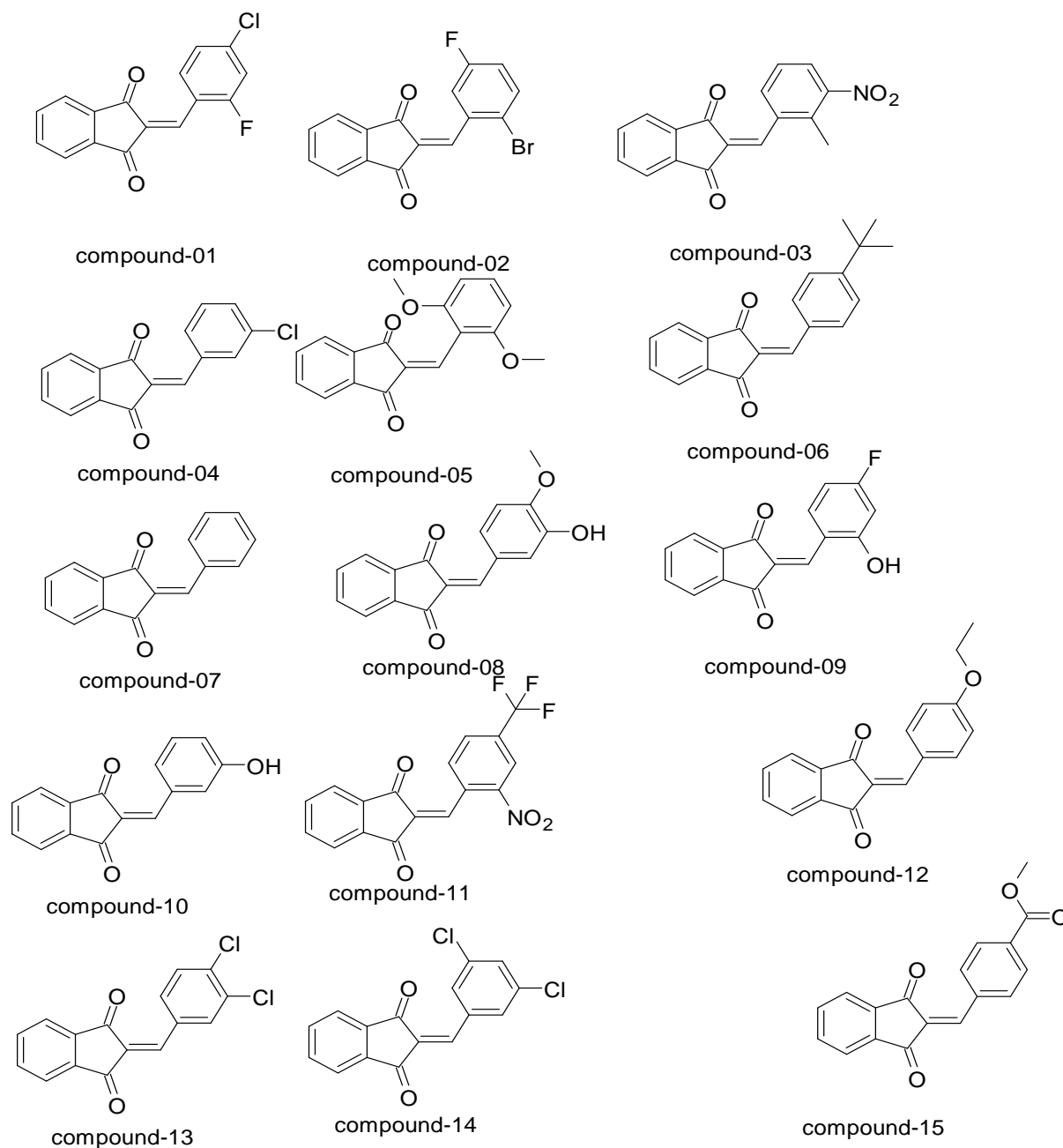
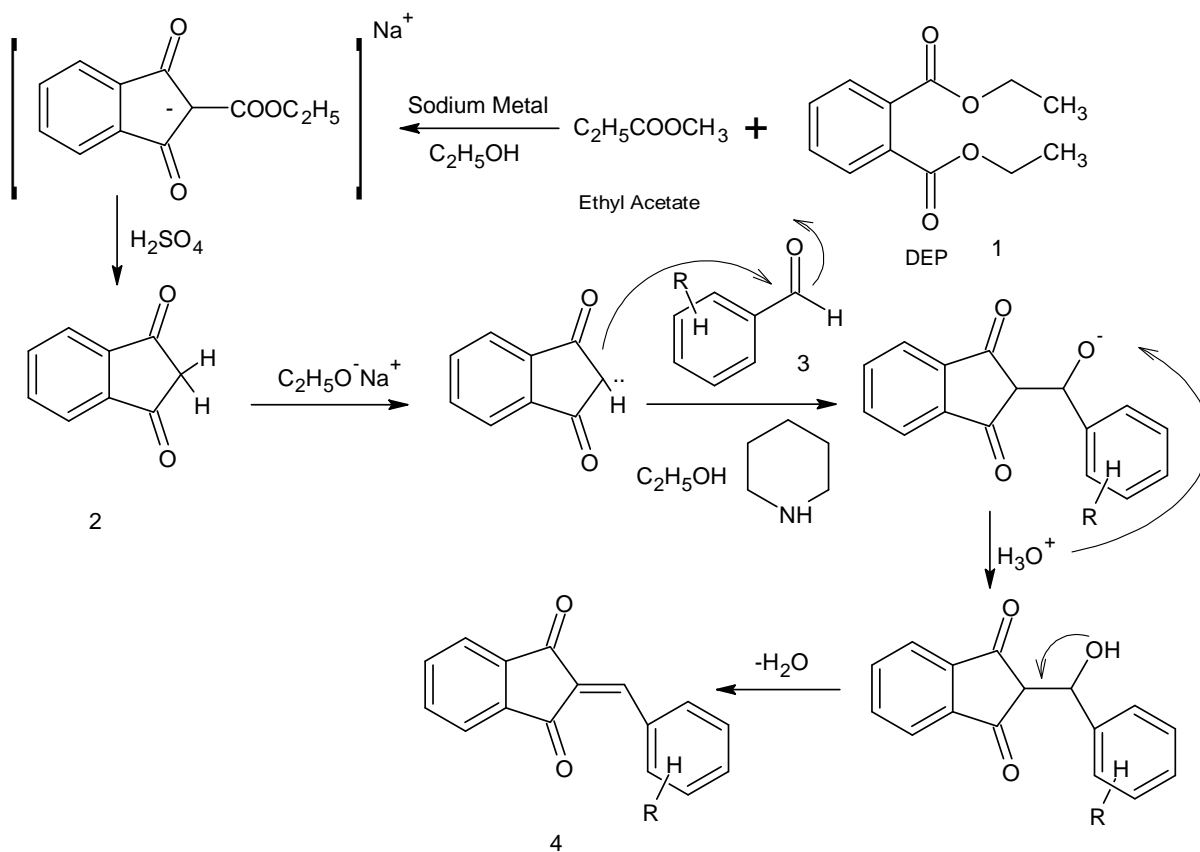


Figure 5: List of 2-(aryl methylene)-(1H)-indane-1, 3-(2H)-diones derivatives for Docking Study



2-arylideneindan-1,3-dione derivatives(1-15)

Figure 6; Scheme 4- Proposed mechanism for the formation of 2-(aryl methylene)-(1H)-indane-1, 3-(2H)-diones

Here's a proposed mechanism of the formation of 2-arylideneindan-1, 3-diones as shown in figure 6:

1. Formation of Enolate Ion: In the first step deprotonation of the 1, 3-dione moiety of an indandione derivative takes place by a strong base, such as an sodium alkoxide ion or a lithium diisopropylamide (LDA), to form the respective enolate ion.
2. Nucleophilic Attack: The enolate ion formed in step one attacks an electrophilic center, which is carbonyl compounds like aldehyde, ketone, or another suitable electrophile, at the α -position relative to the carbonyl group. This creates new carbon-carbon bond and intermediate formed.
3. Tautomerization: The intermediate generated follows tautomerization reaction to form the more stable 2-arylideneindan-1, 3-dione product.

Molecular docking procedure

In recent decades, molecular docking has emerged as a pivotal tool in the realm of computational drug discovery [42]. The relentless pursuit of novel therapeutics to combat diseases necessitates innovative approaches that can expedite the drug development process. Molecular docking, a computational technique, plays a pivotal role in this endeavor by facilitating the prediction of the binding mode and affinity between a small molecule ligand and its target protein [43].

Receptor-ligand docking interaction was carried out to ascertain the possible ligand binding sites and to determine the binding affinity. The docking simulations were achieved using the PyRx software incorporated with AutoDock4.2.

Using ACD-ChemSketch freeware software [44], the structure of desired compounds was drawn, and the corresponding SMILE notations were generated. These SMILE notations were then used to prepare the ligands for docking studies by USCF Chimera tool [45].

The crystal structure of the targeted enzyme (*M. tuberculosis* InhA) with PDB code 6SQ5 having 1.84 Å resolution was retrieved from the Protein Data Bank (<https://www.rcsb.org/>) as shown in figure 8[46].

The 3D ribbon view of *M. tuberculosis* InhA in complex with native ligand is illustrated in Fig. 1. All forms of solvent molecules, ligands, and cofactors imported with the enzyme were removed with the Discovery Studio Visualizer software to achieve good binding interactions between the enzyme (protein) and the ligands (molecules). The enzyme protein was saved in PDB format thereafter, recognized by the PyRx software, and transformed into a macro molecule [47-48].

Using PyRx software, the docking interaction between the targeted enzyme and the protein was computed to evaluate the binding affinities. The interaction types such as electrostatic interaction, hydrogen bonding and hydrophobic interaction were then visualized and analysed using the Discovery Studio Visualizer 16 software [48, 49].

Using PyRx workstation's Autodock Vina, these prepared ligands were docked against the protein, with the grid box placed around the active site of the macromolecule. The active site was identified by the Uniport Chimera tool [50]. The docked ligand-protein complex were saved in PDB format and amino acid interactions were visualized using Biovia Discovery studios [51].

To validate the results of designed derivatives resulting binding mode and binding affinity of native ligand was used with an exhaustiveness value of 8, the three-dimensional grid box [Dimensions (Angstrom) x = 58.7022, size_y = 54.4289, size_z = 64.0864] was modified for molecular docking simulations. Overall molecular docking was undertaken according to reported procedure adopted by S. L. Khan et al [52].

Structural Assessment of the Protein

The Ramachandran plot serves as a visual depiction of the dihedral angles ψ (psi) and ϕ (phi) of amino acid residues within a protein structure. These angles elucidate the rotations occurring around the bonds linking individual amino acid residues within a polypeptide chain. These are utilized for scrutinizing permissible and prohibited zones of these dihedral angles, the plot relies on steric hindrance and additional structural limitations for analysis.

Valuable for evaluating the stereochemical integrity of protein structures, the Ramachandran plot delineates regions where data points are prevalent, signifying energetically permissible conformations for the protein backbone.

Conversely, areas with sparse or absent data points signify energetically unfavorable conformations, offering insights into potential structural discrepancies.

Within the plot, a primary division emerges into three distinct regions, with the "Most favored Region" occupying a prominent space.

This segment encompasses combinations of phi (ϕ) and psi (ψ) angles that denote energetically advantageous states, commonly aligned with the permissible conformations of alpha helices and beta sheets.

An additional area, termed the "Allowed Region," encompasses torsional angle combinations that possess energetic feasibility but occur less frequently compared to those within the most favored region. Conversely, the "Outlier Region" illustrates combinations of phi (ϕ) and psi (ψ) angles that are energetically prohibited. Data points within this region hint at possible structural concerns within the protein, such as steric conflicts or improbable bond geometries. Named after G. N. Ramachandran, an esteemed Indian biophysicist, the plot serves as a tribute to his pioneering contributions in the field [53].

Ramachandran plots were generated for *M. tuberculosis* (InhA) with PDB code 6SQ5 protein using the online webserver Pdbsum database, showing all residue types.

The validation of the modeled docked cancer protein structure involved PROCHECK analysis, wherein the PDB format file containing the docked *M. tuberculosis* (InhA) (6SQ5) ligand was submitted to the PDB SUM online web server.

The results of the PROCHECK analysis were presented as a Ramachandran plot (Fig. 7), offering insights into stereochemical aspects encompassing both main chain and side chain parameters [54-55].

Through this comprehensive analysis, the stereochemical quality of the modeled structure was evaluated, aiding in the assessment of its accuracy and reliability.

Pharmacological Evaluation

Antitubercular Screening

For screening of designed titled compounds 1-15 against *M. tuberculosis* H37RV strain at a concentration from 12.5 to 100 µg/mL in a sterile 96 well plate a nontoxic microplate alamar blue assay (MABA) method employed which is heat stable [56].

To avoid evaporation deionized sterile water (200 µL) was added to the outer perimeter well to 100 µL of Lowenstein-Jensen egg media (LJ media) broth and serial dilutions of the compounds were introduced to the 96 wells plate and incubated at 36 °C for 120 hours.

The sensitive compounds exhibited blue colour after 24 hours incubation against *M. tuberculosis* H37RV strain and the concentrations were recorded.

Lowenstein Jensen media Composition of modified L-J media [57]

Table 1 - Composition of modified L-J media

Composition	Quantity
Potassium dihydrogen phosphate	1.2 g
Magnesium sulphate	0.12 g
Magnesium citrate	0.3
g L-asparagine	1.8 g
Glycerol/Sodium pyruvate	6.0 mL/3.6 g
Distilled water	300 ML
Malachite green (2%)	16 mL
Egg homogenate	500 mL
Benzyl penicillin (1,000,000 IU/ml)	1 mL

The standard strain *Mycobacterium tuberculosis* H37Rv (MTCC-200) were procured from the National Institute of Virology, Pune, India.

M. tuberculosis H37RV Cultures were tested against synthesized and standard drugs. L.J was used as nutrient medium to grow and dilute the drug suspension for the test. The Inoculum size for test strain was adjusted to 1mg/mL. *Mycobacterium tuberculosis* H37Rv [Acid Fast Bacilli] MTCC-200.DMSO was used as diluents to get desired concentration of drugs to test upon Standard bacterial strains [58-59].

Stock solutions were prepared with a concentration of 2000 ug/ml of the synthesized drugs. The drugs found active in various concentrations diluted to obtain 100 µg/mL, 50 µg/mL, 25 µg/mL, and 12.5µg/mL.

Prediction of Activity Spectra for Substances (PASS)

We employed PASS (Prediction of Activity Spectra) to screen for potential properties computationally, including biological activities like cancer-related effects and other relevant activities such as anti-viral and antimicrobial actions. The tool, available at <http://www.way2drug.com/PASSOnline/predict.php>, is specifically tailored to assess the inherent biological potential of drug-like organic compounds. PASS predictions are broad, covering a wide range of activities based on the structural characteristics of organic compounds. Utilizing quantitative structure-activity relationships (SAR), the tool analyzes chemical structures using 2D and/or 3D descriptors, and then generates models from bioactive ligands. It evaluates PASS activity based on structures with a higher probability of activity (Pa), while also considering those predicted as probably inactive (Pi) in pharmacological activity assessments as indicated in table 2[60].

Toxicity Simulation

The LD₅₀ value was predicted using the GUSAR Online tool, with comparative compounds being indan-1, 3-dione based on the molecule's structure [61]. Following this, the Lazar Toxicity Predictions online tool was utilized to assess mutagenicity (in *Salmonella typhimurium*), carcinogenicity (in rats), ability to cross the blood–brain barrier (in humans), and acute toxicity (in Fathead minnow and *Daphnia magna*) as indicated in table 3[62].

In Silico Physicochemical and Pharmacokinetics Studies

Predicting ADMET properties is crucial in the drug discovery and development process, with in silico evaluation models being invaluable tools for scientists in drug design and lead optimization. Physicochemical properties, absorption, distribution, metabolism, toxicity, excretion, and medicinal properties of various substituted 2-(aryl methylene)-(1*H*)-indane-1,3-(2*H*)-diones derivatives are assessed using the online platform ADMET lab 2.0, offering accurate and comprehensive predictions as indicated in table 4[63].

The considered ADMET factors include physicochemical properties, blood-brain barrier (BBB) permeability, Caco-2 permeability, volume of distribution (VD), P-glycoprotein (PGP) substrate status, plasma protein binding, human intestinal absorption (HIA), MDCK permeability, clearance (CL), half-life (T_{1/2}), as well as eye corrosion, eye irritation, respiratory toxicity, AMES toxicity, carcinogenicity, and synthetic accessibility score. This integrated approach aids researchers in evaluating the potential of different 2-(aryl methylene)-(1*H*)-indane-1, 3-(2*H*)-diones derivatives for pharmaceutical use.

During the pre-clinical stages, the in-silico TOX profile acts as a valuable tool for predicting the pharmacological and toxicological properties of drug candidates. The toxicity of synthesized 2-(aryl methylene)-(1*H*)-indane-1, 3-(2*H*)-diones was predicted using the freely accessible online web tool at https://tox-new.charite.de/protox_II/. This resource aids researchers in assessing the potential risks associated with the compounds, offering insights that can inform decision-making processes in drug development [64-65].

The analysis of the BOILED-egg diagram, depicted in Fig.9, indicates that the compound conforms to the acceptable range for standard drugs. Within the diagram, a dot located in the yellow zone suggests that the compound is unaffected by the P-glycoprotein of the CNS system, while a blue dot positioned in the yolk denotes passive permeation through the blood-brain barrier (BBB)[66]. Additionally, the red region indicates the compound's ability to accumulate in the brain. The synthesized ligand and its complexes in this study meet the

established criteria, exhibiting favorable bioavailability. These findings affirm the compound's safety profile, indicating a low likelihood of causing skin allergies. Notably, the drug scores for these compounds are moderate.

4. Result And Discussion

Compound 1: 2-[(4-chloro-2-fluorophenyl)methylidene]-1H-indene-1,3(2H)-dione

Pale yellow solid, yield: 84%, molecular formula: C₁₆H₈ClFO₂, melting point: 174-180⁰C. Elemental analysis (cal.): C (67.03%) H (2.81%) Cl(12.37%) F (6.63%) O (11.16%). FT-IR (neat, cm⁻¹) v_{max}: 3382.53, 3090.66(C-H), 1615.09 (C=O), 730.88(C-Cl), 1160.94(C-F), ¹H NMR (300 MHz, DMSOd₆, chemical shift (ppm)); δ: 8.7-8.8 (m,1H,CH),7.3-7.6(m,4H,Ar-H),7.9-8(m,2H,Ar-H) 8.02-8.04(s,1H,CH),3.12-3.36(s, 1H, CH₃) MS m/z:286.69

Compound 2: 2-[(2-Bromo-5-Fluorophenyl)Methylidene]-1H-Indene-1,3(2H)-Dione

Yellow solid, yield: 85%, molecular formula: C₁₆H₈BrFO₂, melting point: 172-174⁰C. Elemental analysis (cal.): C (58.03%) H (2.44%) Br (24.13%) F (5.74%) O (9.66%). FT-IR (neat, cm⁻¹) v_{max}: 2905(CH), 834(C-F), 1605 (C=O), 680(C-Br), 988(Ar-H), 1555(C=C). ¹H NMR (300MHz, DMSO-d₆, chemical shift (ppm)); δ: 7.40-7.44 (m, 4H, Ar-H), 7.84-7.87 (m, 3H, Ar-H), 8.33-8.35 (m, 1H, CH) MS m/z: 331.13

Compound 3: 2-[(2-methyl-3-nitrophenyl) methylidene]-1H-indene-1, 3(2H)-dione

Yellow solid, yield: 66%, molecular formula: C₁₇H₁₁NO₄, melting point: 222-224⁰C. Elemental analysis (cal.): C (69.62%) H (3.78%) N (4.78%) O (21.82%). FT-IR (neat, cm⁻¹) v_{max}: 2980.45(C-H),1680.88(C=O),1054.87(C-N),1032.69 (Ar-H),¹HNMR (300MHz, DMSO-d₆, chemical shift (ppm));δ: 7.52-7.55(m, 4H, Ar-H), 7.96-8.00 (m, 3H, Ar-H), 3.85 (s, 3H, CH) 8.00-8.12(m,1H,CH) MS m/z : 293.278

Compound 6: 2-[(4-tert-butylphenyl) methylidene]-1H-indene-1, 3(2H)-dione

Pale yellow solid, yield: 81%, molecular formula: C₂₀H₁₈O₂, melting point: 188-190⁰C.Elemental analysis (cal.): C (82.73%) H (6.25%) O (11.02%) FT-IR (neat, cm⁻¹) v_{max}; 3236.93(C-H), 1718.26(C=O), 1664.27 (C=C),1389.46(C-C Stretch),856.239 (Ar-H), 738.603 ¹H NMR (300MHz, DMSO-d₆, chemical shift (ppm));δ: 8.55-8.58(m,1H,CH),8.10 (m, 4H, Ar-H), 7.50 (m, 4H, Ar-H),3.73(s, 9H, 3CH₃)MS m/z:290.36

Compound 8: 2-[(3-hydroxy-4-methoxyphenyl) methylene]-1H-indene-1,3(2H)-dione

Pale yellow powder, yield: 74%, molecular formula:C₁₇H₁₂O₄, melting point: 168-170⁰C. Elemental analysis (cal.): C (72.85%) H (4.32%) O(22.83%); FT-IR (neat, cm⁻¹) v_{max}: 3374.82 cm⁻¹(O-H Stretch), 2990.10 cm⁻¹ (C-H Stretch), 1717.3 cm⁻¹(C=O), 1681.62 cm⁻¹(C=C), 1267 cm⁻¹(C-O), 1036.55 cm⁻¹(C-O Stretch), 994.125 cm⁻¹(Ar-H),883.238 cm⁻¹(C-H Bend),734.746 cm⁻¹(C-H Bend).

¹H NMR (300 MHz, DMSOd₆,chemical shift (ppm)); δ: 8.31(m,1H,CH), 7.92-7.98 (m, 2H, Ar-H), 7.71(s,2H,Ar),7.12-7.14(m,4H,Ar-H),3.91(s,1H,OH),3.53(s,3H,CH₃)MS m/z: 280.27

Compound 9: 2-[(4-fluoro-2-hydroxyphenyl) methylene]-1H-indene-1, 3(2H)-dione

Pale yellow solid, yield: 86 %, molecular formula: C₁₆H₉FO₃, melting point: 162-164⁰C. Elemental analysis (cal.): C (71.64%) H (3.38%) F (7.08%) O (17.89%) FT-IR (neat, cm⁻¹) v_{max}: 3690.48 cm⁻¹ (O-H Stretch) 2980.77 cm⁻¹(C-H Stretch) 1729.83 cm⁻¹(C=O) 1688.37 cm⁻¹ 1606.41 cm⁻¹ (C=C) 1411.64 cm⁻¹(C-F Stretch) 1054.87 cm⁻¹(C-O Stretch) 997.982 cm⁻¹(Ar-H) 731.853 cm⁻¹ (C-H Bend)

^1H NMR (300 MHz, DMSO-d₆, chemical shift (ppm)); δ : 8.55-8.58(m, 1H, CH), 8.41-8.45 (m, 1H, CH), 7.74-8.06(m, 2H, Ar-H), 7.00-7.26(m, 4H, Ar-H), 4.96(s, 1H, OH). MS m/z: 268.23

Compound 11: 2-[[2-nitro-4-(trifluoromethyl) phenyl]methylidene]-1H-indene-1,3(2H)-dione

Pale yellow solid, yield: 72%, molecular formula: C₁₇H₈F₃NO₄, melting point: 235-240^oC. Elemental analysis (cal.): C (58.82%) H (2.30%) F (16.42%) N (4.02%) O (18.42%). FT-IR (neat, cm⁻¹) v_{max}: 3467.38 cm⁻¹ (\equiv C-H stretch), 3000.10 cm⁻¹ (C-H Stretch), 1714.41 cm⁻¹ (C=O), 1448.28 cm⁻¹ (C-H Alkyl), 1386.57 cm⁻¹ (Ar-NO₂), 1266.04 cm⁻¹ (C-O), 1081.87 cm⁻¹ (Ar-H), 876.488 cm⁻¹ (C-F), 730.889 cm⁻¹ (C-C Bend).

^1H NMR (300 MHz, DMSO-d₆, chemical shift (ppm)); δ : 7.95-8.09(m, 4H, Ar-H), 8.55 (m, 1H, CH), 8.11-8.31(m, 3H, CH). MS m/z: 268.24

Compound 12: 2-[(4-ethoxyphenyl) methylene]-1H-indene-1, 3(2H)-dione

Pale yellow needle solid, yield: 86 %, Molecular Formula: C₁₇H₁₂O₃, melting point: 156-158^oC.

Elemental analysis (cal.): C (77.26%) H (4.58%) O (18.16%) FT-IR (neat, cm⁻¹) v_{max}: 3316 cm⁻¹ (\equiv C-H stretch) 2980.45 cm⁻¹ (C-H) 1721.16 cm⁻¹ (C=O) 1663.3 cm⁻¹ (C=C) 1444.42 cm⁻¹ (C-H Alkyl) 1292.07 cm⁻¹ (C-O) 994.125 cm⁻¹ (Ar-H) 878.41 cm⁻¹ (C-H Bend) 727.996 cm⁻¹ (C-C Bend)

^1H NMR (300 MHz, DMSO-d₆, chemical shift (ppm)); δ : 8.52-8.54(m, 1H, CH), 7.91-7.93 (m, 4H, Ar-H), 7.75(s, 4H, Ar-H), 6.92-6.94(m, 3H, CH₃), 3.36-3.40(t, 2H, CH) MS m/z: 264.28

Compound 13: 2-[(3, 4-dichlorophenyl) methylidene]-1H-indene-1, 3(2H)-dione

Pale yellow solid, yield: 69%, molecular formula: C₁₆H₈Cl₂O₂, melting point: 170-175^oC. Elemental analysis (cal.): C (63.39%) H (2.66%) Cl(23.39%) O(10.56%). FT-IR (neat, cm⁻¹) v_{max}: 3680.48 cm⁻¹ 2971.77 cm⁻¹ (C-H Stretch), 2843.52 cm⁻¹ (C-H Stretch) 1687.41 cm⁻¹ (C=O), 1371.14 cm⁻¹ (C=O Stretch), 1054.87 cm⁻¹ 1032.69 cm⁻¹ (Ar-H), 1012.45 cm⁻¹ 738.603 cm⁻¹ (Di-substituted benzene).

^1H NMR (300 MHz, DMSO-d₆, chemical shift (ppm)); δ : 7.73-7.76(m, 4H, Ar-H), 7.87-7.97(m, 2H, Ar-H) 8.00-8.04(s, 1H, CH), 8.64-8.65(m, 1H, CH), MS m/z: 303.29

Compound 15: methyl 4-[(1, 3-dioxo-1, 3-dihydro-2H-inden-2-ylidene) methyl] benzoate

Pale yellow solid, yield: 69%, molecular formula: C₁₈H₁₂O₄, melting point: 170-175^oC. Elemental analysis (cal.): C (73.97%) H (4.14%) O (21.90%) FT-IR (neat, cm⁻¹) v_{max}: 3680.48 cm⁻¹, 2843.52 cm⁻¹ (C-H Stretch), 2971.77 cm⁻¹ (C-H Stretch), 1629.41 cm⁻¹ (C=O), 1346.07 cm⁻¹ (C=O Stretch), 1012.45 cm⁻¹ (Ar-H), 1054.87 cm⁻¹ (C-C (O)-C Stretch) MS m/z: 292.28

^1H NMR (300 MHz, DMSO-d₆, chemical shift (ppm)); δ : 8.79-8.82(m, 1H, CH), 8.02-8.04 (m, 4H, Ar-H), 7.32-8.01(m, 4H, Ar-H), 3.36-3.73(s, 3H, CH₃)

Molecular docking studies

To determine the binding affinities and binding energy scores of the synthesized derivatives interactions of amino acid residues with in the active pocket of protein have been studied. The docking simulation results proves that a significant proportion of the derivatives shown robust binding scores and remarkable binding affinity energy.

The comparison of binding affinities of all the docked derivatives carried out with the binding mode of native ligand present in the crystal structure of M. tuberculosis InhA enzyme (PDB ID: 6SQ5).

Notably, compound 11 have the best binding energy of -9.2 kcal/mol. The best configuration of compound 11 was chosen for further study, reflecting results of analysis indicating bonding and non-bonding interactions and formed two conventional hydrogen bond interactions with GLY192. It has exhibited hydrophobic interactions [Pi-Pi stacked, Pi-alkyl, Halogen (Fluorine)] with amino acids PHE149, PRO193, MET199, ILE215, PRO193, MET199 showing bond length 4.06816, 4.75824, 4.43885, 4.86179, 5.43103, 4.60512 \AA respectively.

Compound 9 displayed -9.5 kcal/mol binding affinity and formed one conventional hydrogen bond with GLY96. It has formed many hydrophobic interactions (Pi-sigma, Pi-Pi stacked, Pi-alkyl) with amino acids residues ILE95, ILE122, PHE41, PHE41, VAL65, ILE95 showing bond length 3.73999, 3.89114, 3.73151, 4.62143, 4.92791, 4.99177 \AA .

Compound 6 showed -9.6 kcal/mol binding affinity and lacks conventional hydrogen bond interaction but shown many hydrophobic bonds (Pi-Sigma, Pi-Pi Stacked, Pi-Alkyl) with amino acid residues ILE95, PHE41, VAL65, ILE95, ILE122, ILE16 exhibit 3.54876, 3.81165, 4.67903, 4.78472, 4.57524, 5.43011 \AA bond length respectively.

Compound 1 exhibited -9.9 kcal/mol docking score and formed none of conventional hydrogen bonds but exhibit hydrophobic interactions (Pi-sigma, Halogen, Pi-Pi stacked and Pi-alkyl) with ILE95, ILE122, PHE41, PHE41, ALA198, VAL65, ILE95, ILE16 showing bond length 3.65928, 3.96784, 3.72912, 4.61041, 3.8642, 4.80754, 4.94907, 5.24967 \AA respectively.

The residues that interact with compound 13 are as follows: ILE95, ILE122, PHE41, ALA198, VAL65, ILE122 and ILE16 forms hydrophobic interactions (Pi-Sigma, Pi-Pi Stacked, Alkyl, Pi-Alkyl).

Compounds 3 formed two conventional hydrogen bond with LYS165, ILE194 and have binding affinity -9.1 kcal/mol. It has developed many hydrophobic interactions (Pi-Pi Stacked, Pi-Pi Stacked, Pi-Alkyl) with amino acid residues PHE149, PRO193, MET199, and ILE215 respectively.

Compounds 5 formed one conventional hydrogen bond with GLY96 and have binding affinity -8.9 kcal/mol. The amino acid residues forms hydrophobic interactions (Pi-Sigma, Pi-Pi Stacked, Pi-Alkyl) with drug are ILE95, PHE41, VAL65, ILE95, ILE122, ILE16 respectively.

Therefore from this investigation we have selected 1,2,3,6,8,11,12,13,15 for the wet lab synthesis and spectral study.

The Ramachandran plot generated for enzyme 6SQ5 using PROCHECK server describes different coloured regions / shading on phi-psi plot. The protein at Ramachandran statistics shows 267 total number of residues, most favoured regions (A, B, L) of residues 206 with a percentage of 91.6 %, with allowed regions (a,b,l, p) 16 residues of 7.1 %, Generously allowed regions (a,b,l,p) 0 residues in 0.0 %. Over all total Non-glycine and non-proline residues 225 of 100 %. In addition to this Proline residues 13, Glycine residues 28, End-residues (excl. Gly-and Pro) 1, overall total number of residues present in the 267.

The analysis of the predicted structure affords solid evidence that the predicted 3D structure of the protein is of excellent quality. The Ramachandran plot generated using PROCHECK statistics are summarized in Figure 7.

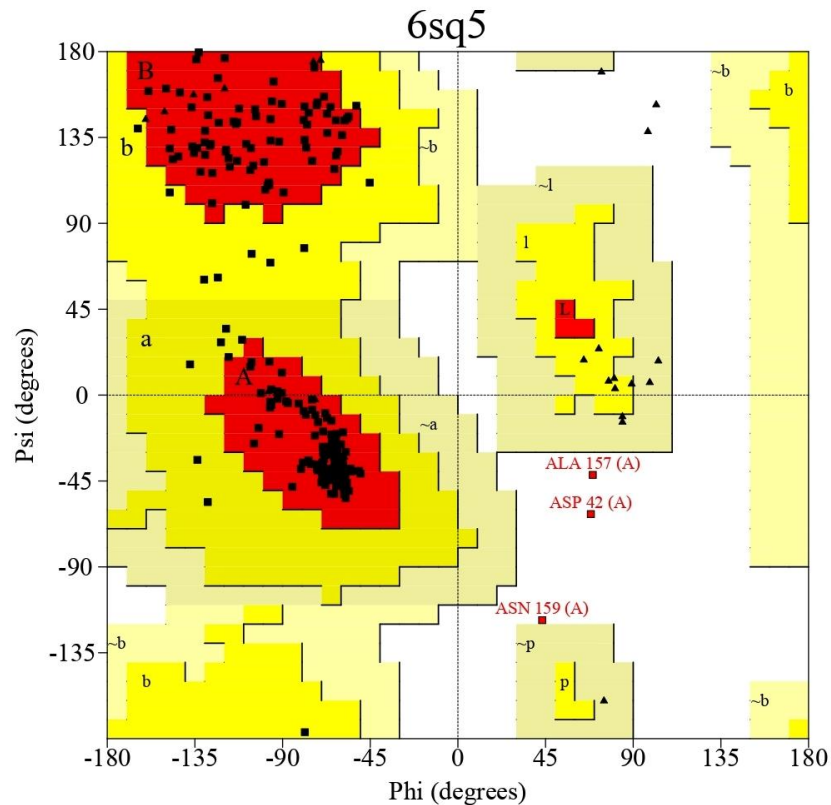


Fig. 7. Ramachandran plot of 6SQ5 showing 91.6 % of amino acid residues in the core region into binding site of *M. tuberculosis* InhA protein

Plot statistics

Residues in most favoured regions [A,B,L]	206	91.6%
Residues in additional allowed regions [a,b,l,p]	16	7.1%
Residues in generously allowed regions [~a,~b,~l,~p]	0	0.0%
Residues in disallowed regions	3	1.3%

Number of non-glycine and non-proline residues	225	100.0%
Number of end-residues (excl. Gly and Pro)	1	
Number of glycine residues (shown as triangles)	28	
Number of proline residues	13	

Total number of residues	267	

Based on an analysis of 118 structures of resolution of at least 2.0 Angstroms and R-factor no greater than 20%, a good quality model would be expected to have over 90% in the most favoured regions.

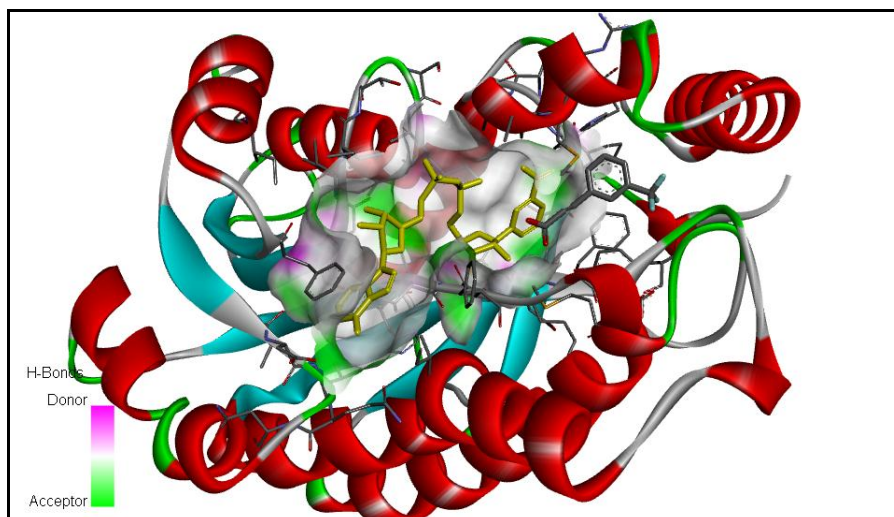
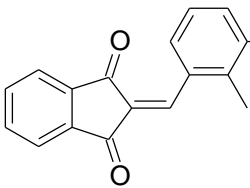
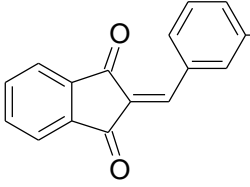
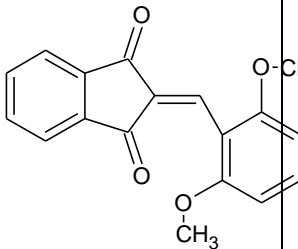
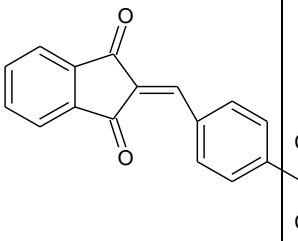
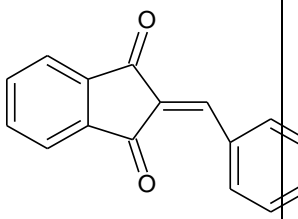
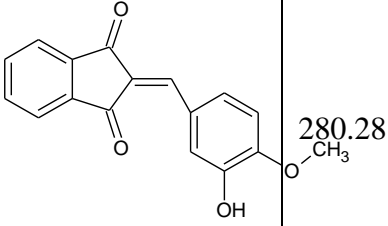
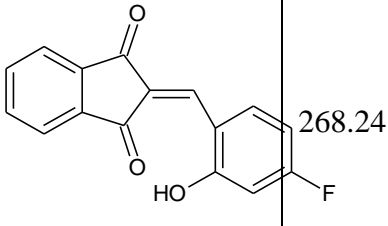
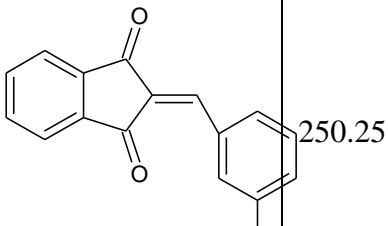
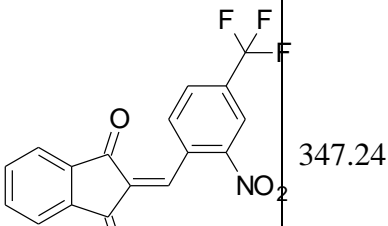
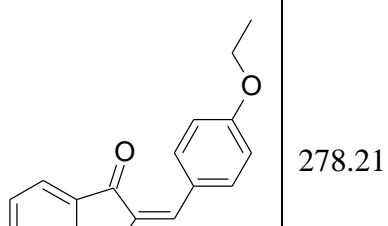


Fig.8.The 3D ribbon view of *M. tuberculosis* InhA in complex with NAD⁺ and 3-[3-(trifluoro methyl) phenyl] prop-2-enoic acid (6SQ5)

Table 2. Physical Characterization of synthesized compound (1-15)

Sr. No.	IUPAC Name	Chemical Structure	Mole. Wt	Percentage Yield	Docking score (kcal/mol)
1	2-[(4-chloro-2-fluorophenyl)methylidene]-1 <i>H</i> -indene-1,3(2 <i>H</i>)-dione		286.69	84	-9.2
2	2-[(2-bromo-5-fluorophenyl)methylidene]-1 <i>H</i> -indene-1,3(2 <i>H</i>)-dione		331.14	85	-9.2

3	2-[(2-methyl-3-nitrophenyl)methylidene]-1 <i>H</i> -indene-1,3(2 <i>H</i>)-dione		293.28	66	-9.1
4	2-[(3-chlorophenyl)methylidene]-1 <i>H</i> -indene-1,3(2 <i>H</i>)-dione		268.7	75	-9
5	2-[(2,6-dimethoxyphenyl)methylidene]-1 <i>H</i> -indene-1,3(2 <i>H</i>)-dione		294.30	79	-8.9
6	2-[(4- <i>tert</i> -butylphenyl)methylidene]-1 <i>H</i> -indene-1,3(2 <i>H</i>)-dione		290.36	81	-9.6
7	2-benzylidene-1 <i>H</i> -indene-1,3(2 <i>H</i>)-dione		234.25	82	-8.8

8	2-[(3-hydroxy-4-methoxyphenyl)methylidene]-1 <i>H</i> -indene-1,3(2 <i>H</i>)-dione		280.28	74	-9.1
9	2-[(4-fluoro-2-hydroxyphenyl)methylidene]-1 <i>H</i> -indene-1,3(2 <i>H</i>)-dione		268.24	86	-9.5
10	2-[(3-hydroxyphenyl)methylidene]-1 <i>H</i> -indene-1,3(2 <i>H</i>)-dione		250.25	72	-9.1
11	2-[[2-nitro-4-(trifluoromethyl)phenyl]methylidene]-1 <i>H</i> -indene-1,3(2 <i>H</i>)-dione		347.24	86	-9.9
12	2-[(4-ethoxyphenyl)methylidene]-1 <i>H</i> -indene-1,3(2 <i>H</i>)-dione		278.21	79	-8.9

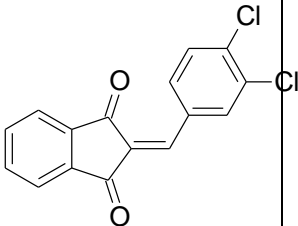
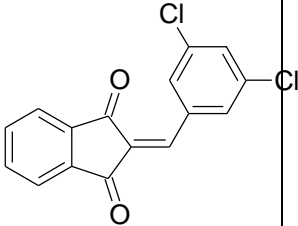
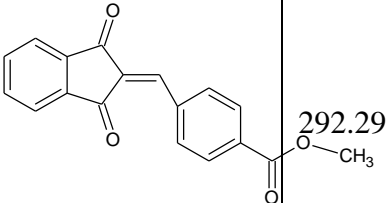
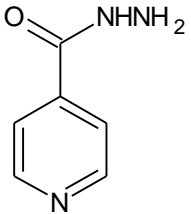
13	2-[(3,4-dichlorophenyl)methylene]-1 <i>H</i> -indene-1,3(2 <i>H</i>)-dione		303.14	69	-9.3
14	2-[(3,5-dichlorophenyl)methylene]-1 <i>H</i> -indene-1,3(2 <i>H</i>)-dione		303.14	71	-8.9
15	methyl 4-[(1,3-dioxo-1,3-dihydro-2 <i>H</i> -inden-2-ylidene)methyl]benzoate		292.29	80	-9.1
16	Pyridine-4-carbohydrazide (Isoniazide)		137.14	-	-5.8

Table 3. Molecular interactions of Indane -1, 3 Dione derivatives with 6SQ5

Comp. No	Distance	Category	Type of Interaction	No. of H-Bond	Amino acid residue
Comp-1	3.46059	Halogen	Halogen (Fluorine)	0	N:UNL1:O - N:UNL1:F
	3.65928	Hydrophobic	Pi-Sigma		ILE95
	3.96784	Hydrophobic	Pi-Sigma		ILE122

	3.72912	Hydrophobic	Pi-Pi Stacked		PHE41
	4.61041	Hydrophobic	Pi-Pi Stacked		PHE41
	3.8642	Hydrophobic	Alkyl		ALA198
	4.80754	Hydrophobic	Pi-Alkyl		VAL65
	4.94907	Hydrophobic	Pi-Alkyl		ILE95
	5.24967	Hydrophobic	Pi-Alkyl		ILE16
Comp-2	3.78248	Hydrophobic	Pi-Sigma	0	ILE95
	3.88314	Hydrophobic	Pi-Sigma		ILE122
	3.76654	Hydrophobic	Pi-Pi Stacked		PHE41
	4.56831	Hydrophobic	Pi-Pi Stacked		PHE41
	3.72131	Hydrophobic	Alkyl		ILE16
	4.86426	Hydrophobic	Pi-Alkyl		VAL65
	4.95238	Hydrophobic	Pi-Alkyl		ILE95
	5.20649	Hydrophobic	Pi-Alkyl		ILE16
Comp -3	2.77841	Hydrogen Bond	Conventional Hydrogen Bond	2	LYS165
	2.34339	Hydrogen Bond	Conventional Hydrogen Bond		ILE194
	3.7569	Other	Pi-Sulfur		MET199
	4.43052	Hydrophobic	Pi-Pi Stacked		PHE149
	4.40643	Hydrophobic	Pi-Pi Stacked		PHE149
	5.19988	Hydrophobic	Pi-Alkyl		PRO193
	5.33453	Hydrophobic	Pi-Alkyl		MET199
	4.93067	Hydrophobic	Pi-Alkyl		ILE215
	5.09629	Hydrophobic	Pi-Alkyl		PRO193
Comp -4	3.5897	Hydrophobic	Pi-Sigma	0	ILE95
	3.83636	Hydrophobic	Pi-Sigma		ILE122
	3.70483	Hydrophobic	Pi-Pi Stacked		PHE41
	4.5656	Hydrophobic	Pi-Pi Stacked		PHE41
	4.89657	Hydrophobic	Pi-Alkyl		VAL65
	5.15552	Hydrophobic	Pi-Alkyl		ILE95
	5.42873	Hydrophobic	Pi-Alkyl		ILE122
	5.40981	Hydrophobic	Pi-Alkyl		ILE16
Comp -5	2.38816	Hydrogen Bond	Conventional Hydrogen Bond	1	GLY96
	3.74988	Hydrophobic	Pi-Sigma		ILE95
	3.79877	Hydrophobic	Pi-Pi Stacked		PHE41
	4.65174	Hydrophobic	Pi-Pi Stacked		PHE41
	4.7695	Hydrophobic	Pi-Alkyl		VAL65
	4.7787	Hydrophobic	Pi-Alkyl		ILE95
	4.58236	Hydrophobic	Pi-Alkyl		ILE122
	5.06896	Hydrophobic	Pi-Alkyl		ILE16
Comp -6	3.54876	Hydrophobic	Pi-Sigma	0	ILE95
	3.81165	Hydrophobic	Pi-Pi Stacked		PHE41
	4.71845	Hydrophobic	Pi-Pi Stacked		PHE41
	4.67903	Hydrophobic	Pi-Alkyl		VAL65
	4.78472	Hydrophobic	Pi-Alkyl		ILE95
	4.57524	Hydrophobic	Pi-Alkyl		ILE122
	5.43011	Hydrophobic	Pi-Alkyl		ILE16

Comp -7	3.6197	Hydrophobic	Pi-Sigma	0	ILE95
	3.87355	Hydrophobic	Pi-Sigma		ILE122
	3.66971	Hydrophobic	Pi-Pi Stacked		PHE41
	4.59076	Hydrophobic	Pi-Pi Stacked		PHE41
	4.94939	Hydrophobic	Pi-Alkyl		VAL65
	5.15017	Hydrophobic	Pi-Alkyl		ILE95
	5.44049	Hydrophobic	Pi-Alkyl		ILE122
Comp -8	3.60577	Hydrophobic	Pi-Sigma	0	ILE95
	3.86704	Hydrophobic	Pi-Sigma		ILE122
	3.6593	Hydrophobic	Pi-Pi Stacked		PHE41
	4.63241	Hydrophobic	Pi-Pi Stacked		PHE41
	5.01112	Hydrophobic	Pi-Alkyl		VAL65
	5.16015	Hydrophobic	Pi-Alkyl		ILE95
	5.44785	Hydrophobic	Pi-Alkyl		ILE122
Comp -9	2.22533	Hydrogen Bond	Conventional Hydrogen Bond	1	GLY96
	3.73999	Hydrophobic	Pi-Sigma		ILE95
	3.89114	Hydrophobic	Pi-Sigma		ILE122
	3.73151	Hydrophobic	Pi-Pi Stacked		PHE41
	4.62143	Hydrophobic	Pi-Pi Stacked		PHE41
	4.92791	Hydrophobic	Pi-Alkyl		VAL65
	4.99177	Hydrophobic	Pi-Alkyl		ILE95
Comp -10	3.60696	Hydrophobic	Pi-Sigma	0	ILE95
	3.85075	Hydrophobic	Pi-Sigma		ILE122
	3.67284	Hydrophobic	Pi-Pi Stacked		PHE41
	4.58972	Hydrophobic	Pi-Pi Stacked		PHE41
	4.96457	Hydrophobic	Pi-Alkyl		VAL65
	5.17582	Hydrophobic	Pi-Alkyl		ILE95
	5.41836	Hydrophobic	Pi-Alkyl		ILE122
Comp -11	3.21504	Hydrogen Bond	Conventional Hydrogen Bond	2	GLY192
	2.26697	Hydrogen Bond	Conventional Hydrogen Bond		N:UNL1:H - N:UNL1:O
	3.61348	Halogen	Halogen (Fluorine)		GLU219
	4.06816	Hydrophobic	Pi-Pi Stacked		PHE149
	4.75824	Hydrophobic	Alkyl		PRO193
	4.43885	Hydrophobic	Alkyl		MET199
	4.86179	Hydrophobic	Alkyl		ILE215
	5.43103	Hydrophobic	Pi-Alkyl		PRO193
	4.60512	Hydrophobic	Pi-Alkyl		MET199
Comp -12	3.60558	Hydrophobic	Pi-Sigma	0	ILE95
	3.8889	Hydrophobic	Pi-Sigma		ILE122
	3.66415	Hydrophobic	Pi-Pi Stacked		PHE41
	4.57446	Hydrophobic	Pi-Pi Stacked		PHE41
	4.92365	Hydrophobic	Pi-Alkyl		VAL65
	5.1515	Hydrophobic	Pi-Alkyl		ILE95
	5.46458	Hydrophobic	Pi-Alkyl		ILE122

	5.43407	Hydrophobic	Pi-Alkyl		ILE16
Comp -13	3.61269	Hydrophobic	Pi-Sigma	0	ILE95
	3.84798	Hydrophobic	Pi-Sigma		ILE122
	3.68015	Hydrophobic	Pi-Pi Stacked		PHE41
	4.56706	Hydrophobic	Pi-Pi Stacked		PHE41
	4.45103	Hydrophobic	Alkyl		ALA198
	4.93384	Hydrophobic	Pi-Alkyl		VAL65
	5.17865	Hydrophobic	Pi-Alkyl		ILE95
	5.40379	Hydrophobic	Pi-Alkyl		ILE122
	5.49289	Hydrophobic	Pi-Alkyl		ILE16
Comp -14	3.99427	Hydrophobic	Pi-Sigma	0	ILE16
	3.91303	Hydrophobic	Pi-Sigma		ILE95
	3.89153	Hydrophobic	Pi-Sigma		ILE122
	3.82937	Hydrophobic	Pi-Pi Stacked		PHE41
	4.65705	Hydrophobic	Pi-Pi Stacked		PHE41
	4.27566	Hydrophobic	Alkyl		ILE16
	4.97339	Hydrophobic	Pi-Alkyl		VAL65
	4.80664	Hydrophobic	Pi-Alkyl		ILE95
Comp -15	3.58121	Hydrophobic	Pi-Sigma	0	ILE95
	3.91412	Hydrophobic	Pi-Sigma		ILE122
	3.70114	Hydrophobic	Pi-Pi Stacked		PHE41
	4.6409	Hydrophobic	Pi-Pi Stacked		PHE41
	4.88321	Hydrophobic	Pi-Alkyl		VAL65
	5.04281	Hydrophobic	Pi-Alkyl		ILE95
	5.47329	Hydrophobic	Pi-Alkyl		ILE16

Anti-tubercular Activity

Screening of 4-halogen substituted 2 aryl Indane-1, 3-dione derivatives (01-15) against Mycobacterium tuberculosis H37Rv

As previously described in materials and methods 4-halogen substituted 2 aryl Indane-1, 3-dione derivatives were synthesized. All the compounds thus obtained were screened against Mycobacterium tuberculosis H37Rv strain, MIC values were found to be between 4.5µM to 167µM.

Different groups at 14th and 16th position of indane-1, 3-dione derivatives influenced the inhibition of Mycobacterium strains. Compound 1, 10, 11, 12, 15 showed good activity whereas compound numbers 2,3,4,5,6,7,8 and 14 showed moderate activity and 7, 8 showed less activity as compared to standard. The MIC values are listed below in the table.

The drugs found active in primary screening were similarly diluted to obtain 100 µg/mL, 50 µg/mL, 25 µg/mL, and 12.5µg/mL concentrations.

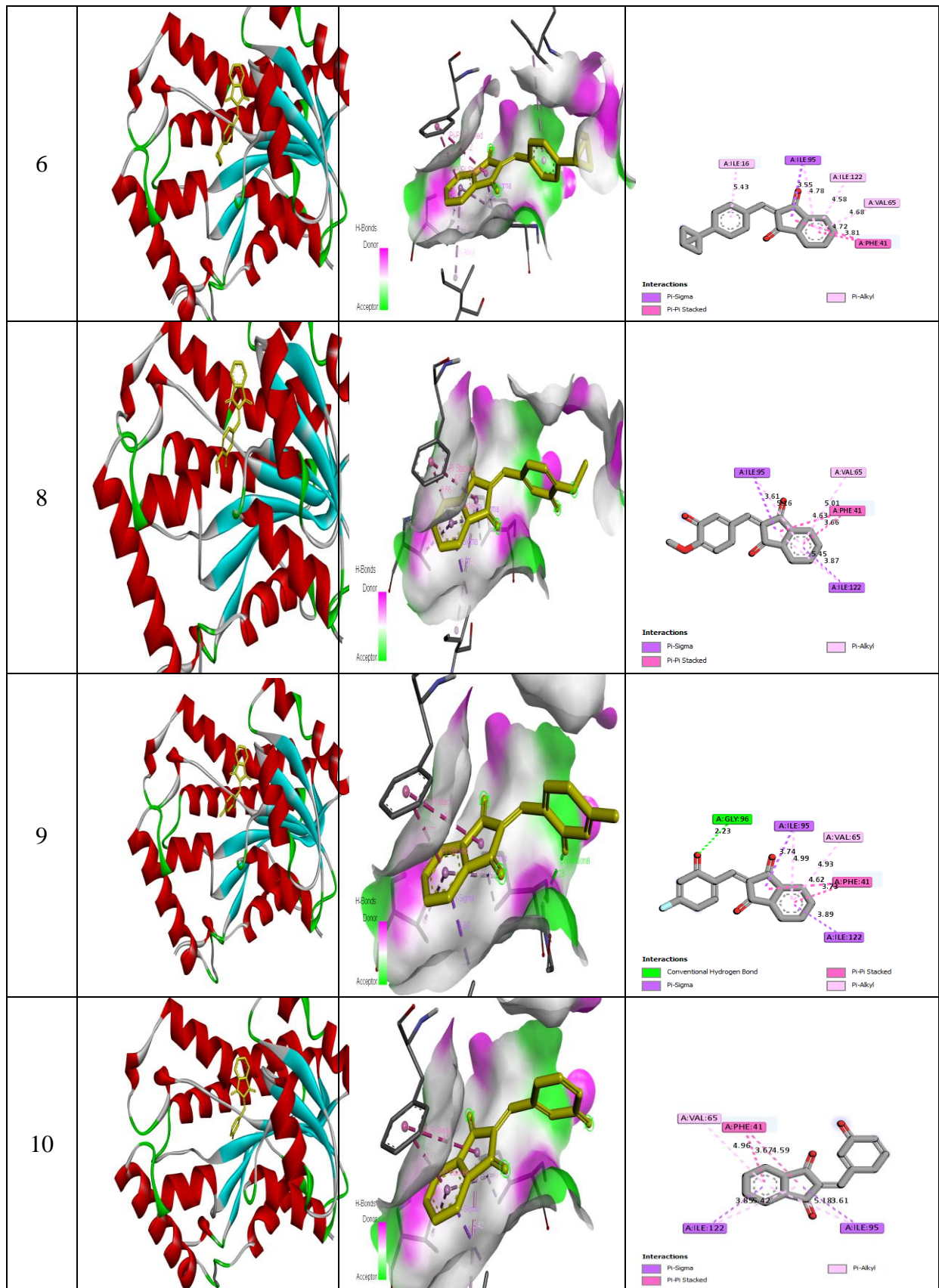
Table 4: Antitubercular activity of synthesized Compounds

Compound	Anti- tubercular activity: MIC(µM)			
	100 µg/mL	50 µg/mL	25 µg/mL	12.5µg/mL
STD	168.7	112.4	85.2	65.2
1	124.5	81.4	65.8	34.5
2	111.2	75.4	58.2	31.2
3	109.7	81.2	51.6	29.5
4	121.5	78.5	62.5	30.6

5	107.9	79.6	49.5	28.3
6	106.9	78.2	47.9	26.3
7	65.2	30.1	17.5	11.8
8	61.4	28.9	16.5	12.4
9	114.2	75.1	63.2	60.8
10	104.2	77.6	64.2	61.3
11	112.3	74.3	68.1	66.2
12	119.5	91.2	74.3	56.2
13	110.9	72.3	66.2	51.4
14	97.2	71.2	48.2	34.2
15	120.5	89.2	75.2	56.3

Three-dimensional and two-dimensional docking poses of the most active compounds

Co mp ID	Ligand protein interaction	3D	2D
1			
2			
3			



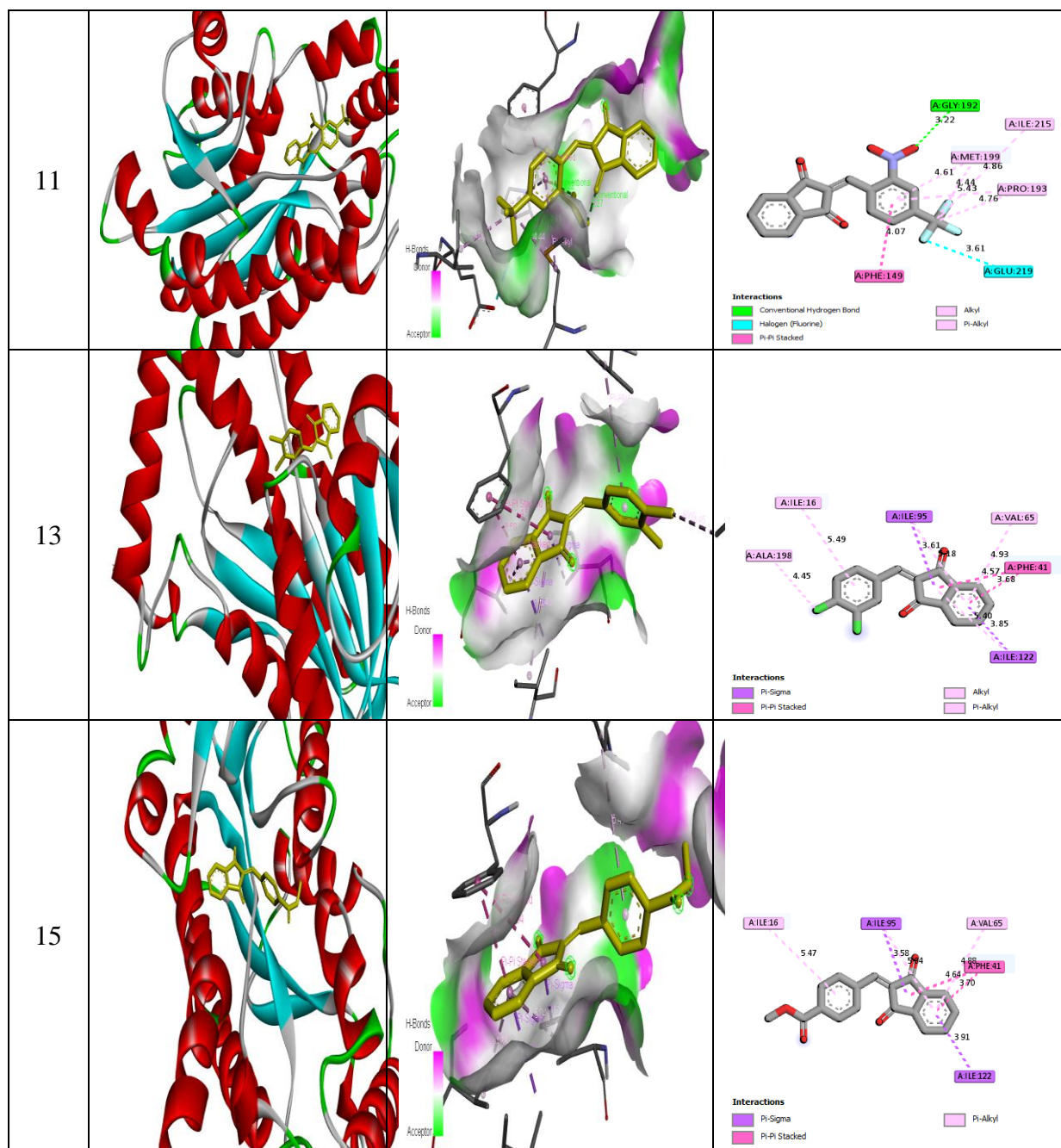


Figure 9: A molecular interaction between Indane 1,3-dione derivatives and 6SQ5 : (b) Binding position in the active site of 6SQ5; (c) the type of interaction of Compounds that binds to the amino acids of 6SQ5.

The determined LD₅₀ values are shown in Table 6

Table 6-In silico LD₅₀ values are determined and the compounds are classified according to their acute toxicity.

Compound	LD ₅₀ *	Toxicity Class**	Compound	LD ₅₀ *	Toxicity Class**
1	530.4	Harmful	9	916.9	Harmful
2	821.9	Harmful	10	2207.0	Unclassified
3	2206.0	Unclassified	11	960.0	Harmful
4	1140.0	Harmful	12	2490.0	Unclassified
5	2116.0	Unclassified	13	685.3	Harmful

6	1930.0	Harmful	14	929.9	Harmful
7	1787.0	Harmful	15	3087.0	Unclassified
8	2608.0	Unclassified	Isoniazide	899.7	Toxic

* After oral administration, the lethal dose causing death of half of the studied rat population is measured in milligrams per kilogram of body weight

** Classification of a chemical used in the European community based on its oral toxicity

Table 7- Pass prediction table

Sr. No	Therapeutic Activity	Probability of activity (Pa)	Probability of inactivity (Pi)
1.	Ubiquinol-cytochrome-c reductase inhibitor	0,824	0,025
2.	Membrane permeability inhibitor	0,637	0,068
3.	NADPH-ferrihemoprotein reductase inhibitor	0,518	0,021
4.	P-benzoquinone reductase (NADPH) inhibitor	0,461	0,026
5.	HIF1A expression inhibitor	0,468	0,069
6.	Histidine kinase inhibitor	0,407	0,050
7.	Apoptosis agonist	0,417	0,066
8.	CYP2A1 substrate	0,395	0,081
9.	Antituberculosic	0,310	0,065
10.	NAD ⁺ kinase inhibitor	0,222	0,027
11.	L-ascorbate peroxidase inhibitor	0,188	0,023
12.	Chlordecone reductase inhibitor	0,308	0,149
13.	Antihemorrhagic	0,179	0,029
14.	2-Dehydropantoate 2-reductase inhibitor	0,302	0,157
15.	Antimutagenic	0,205	0,075
16.	CYP1A inducer	0,204	0,081
17.	Aldehyde dehydrogenase inhibitor	0,174	0,057
18.	Membrane integrity agonist	0,271	0,217
19.	CYP2C12 substrate	0,241	0,204
20.	Aryl-alcohol dehydrogenase (NADP ⁺) inhibitor	0,110	0,102

Analysis of the spectrum of biological activity

With the aid of an online PASS server, the synthetic Indane 1, 3 dione derivatives were ascertained. According to Table 7, compound 11, which is a 2- { [2-nitro- 4-(trifluoromethyl) phenyl] methylidene} -1H-indene -1,3(2H)- dione, showed the best chance of inhibiting Ubiquinol-cytochrome-c reductase enzyme systems in body . Drug-like qualities were discovered during the assessment of the potential activities of indane 1,3-dione derivatives. These include suppression of aryl-alcohol dehydrogenase (NADP⁺)

(Pa: 0.110, Pi: 0.102), antitubercular activity (Pa: 0.310, Pi: 0.065), antihemorrhagic activity (Pa: 0.179, Pi: 0.029), and antimutagenic effects (Pa: 0.205, Pi: 0.075). Table 7 also includes a list of other activities whose odds are higher than 70%. Compound 11 satisfied the majority of the requirements for drug similarity, as shown by the bioavailability radar map, with the exception of log P and log S, which have an impact on membrane permeability.

Moreover, the Pan Assay Interference Compounds (PAINS) projected that every compound would have a single warning, which is required to tolerate non-selective behavior and erratic reactivity with target proteins.

The series of compounds shown in Table 8's drug-likeness prediction research all met Lipinski, Bioavailability score, and Drug-likeness rule criteria, with the exception of 1, 2, 4, 6, 9, 12, 13, 14, and 15 that did not meet the Pfizer rule.

The best range for each property (lipophilicity: Log P between 2.634-4.583 and 4.81; size: MW between 234.07 and 347.04 g/mol; polarity: TPSA between 92 and 142⁰A²; solubility: log S not exceeding 6; etc.) is represented by the area that is colored pink. The sp³ is suggested by the carbon content detected between 0.056-0.111.

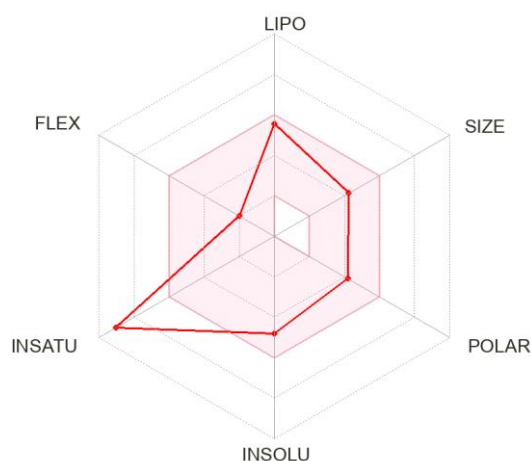


Fig 10. Swiss ADME - bioavailability radar models of 2-[[2-nitro-4-(trifluoromethyl)phenyl]methylidene]-1H-indene-1,3(2H)-dione (Compound 11)

ADMET properties:

All synthesized compounds exhibit a molecular weight < 500, which improves drug transport and rate of absorption as well as penetration across the biological membrane. All of these Indane 1,3dione derivatives topological polar surface areas (TPSA) were less than 140 Å².

Log P values indicating lipophilic behaviour which shows the entire Indane 1,3dione derivative examined found within the 2.634–4.583 range, which is acceptable as per Lipinski's rule of five. The results of physicochemical properties indicate that newer synthesized Indane 1, 3-dione derivatives are within the acceptable range, as shown by the bioavailability radar diagram (Figure 10&12).

The parameters for Indane 1, 3-dione derivatives' are obtained using the online web server ADMET Lab 2.0 the utilization of CaCo-2 cells, which are generated from human colon epithelial cells, is a widespread approach to estimate the absorption of drugs across human digestive tract. On the other hand, Madin Darby Canine Kidney (MDCK) cells are of particular value in evaluating the permeability of drug molecules, as they possess a shorter growing time in comparison to CaCo-2 cells.

Caco-2 cell permeability has been a crucial indicator when compounds projected value found > 5 log cm s⁻¹ (green), it is considered to fit proper Caco-2 permeability. Based on this rule,

we found that the Indane 1, 3 dione derivatives (1-15) have a fit proper Caco-2 permeability within the range of -4.709 to $-4.997 \log \text{ cm s}^{-1}$. Hence indicating favorable membrane permeability characteristics for these compounds. All Indane 1, 3-dione derivatives' exhibited favorable MDCK cell permeability, suggesting a heightened likelihood of renal cell-mediated removal. In terms of Plasma glycoprotein (PGP) inhibitors and PGP substrates, all compounds were shown to be PGP inhibitors and compounds 5, 6 and 8 act as substrates. The calculated values for human intestinal absorption (HIA) reflecting that all compounds effectively absorbed through the intestinal membrane. The analysis of plasma protein binding (PPB) property is an important factor in evaluating the safety profile of newer medications. Drugs with a high PPB value ($>90\%$) often exhibit a narrow therapeutic index, indicating a smaller margin of safety. Medications with low values of PPB value are generally considered to be safer to use. In the current study, it was shown that all compounds 12-15 had low plasma protein binding (PPB) values, indicating a wide therapeutic index for these compounds except compound 1 showing 100.81% binding. Compounds that have CBrain/CBlood values greater than 1 are categorized as possessing central nervous system (CNS) activity, whereas compounds with CBrain/CBlood values below 1 are characterized as lacking CNS activity. Compounds acting over central nervous system (CNS) have properties to cross Blood-Brain Barrier (BBB) and produces adverse effects on the central nervous system. Based on the data provided in Table 8, it can be seen compounds 3 and 14 does not cross BBB, as a result, the compounds exhibit a lack of neurotoxicity. Low value of synthetic accessibility SAscore < 6 indicating all the compounds easy to synthesize. Here SA values lies in between 1.775 - 2.271 proving all the derivatives are easy to synthesize.

Volume of distribution (VD) reflects concentration of drug administered that is present in circulation and describes in vivo distribution of drugs. All the compounds VD is in the range of 0.554 - 0.688 L/Kg indicating excellent distribution in body fluids and uptake amount in tissues.

ADMETlab 2.0 website <https://admetmesh.scbdd.com/service/evaluation/cal> were employed to calculate toxic properties of Indane 1,3 dione derivatives **1-15** and all the properties summed in Table 9. Study of human liver hepatotoxicity (H-HT) is one of important factor to predict safety properties of newer drugs. Predicted value ranging between 0.0 - 0.3 shows no toxicity, 0.3 - 0.7 shows medium toxicity to hepatic cells and a strong toxicity observed at value of 0.7 - $1.0(++)$. Compound 5 gives result of 0.3 lacks hepatic toxicity whereas compounds 1,2,3,4,9,11 have HT value 0.862 indicating toxic nature. Rest of compounds have 0.5 - 0.7 HT values proven medium toxicity to liver cells. Toxicity prediction comprises compound 4 and 6, which had lower predicted values of 0.78 and 0.793 , respectively, are categorised as non-carcinogenic. Whereas other has moderate to exceptional carcinogenic properties with predicted ranges of 0.805 - 0.931 .

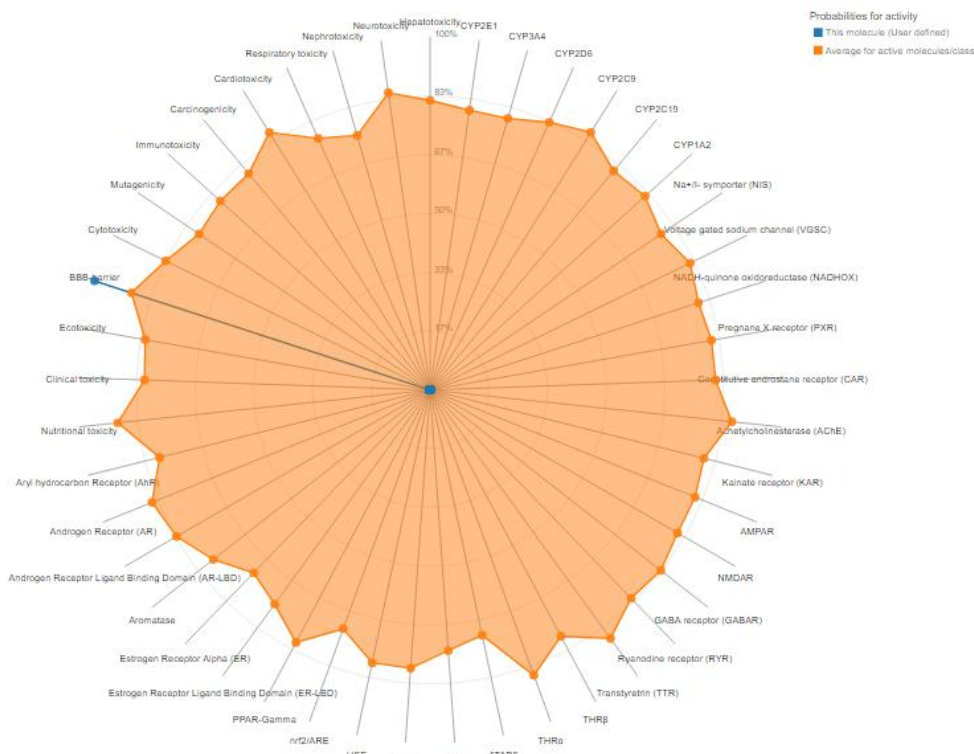


Fig. 11. The in-silico Tox profile of 2-[[2-nitro-4-(trifluoromethyl) phenyl] methylene]-1H-indene-1,3(2H)-dione(Compound 11)

Metabolism pattern of target compounds with cytochrome P450 mono-oxidase enzymes namely CYP1A2, CYP2C19, CYP2C9, CYP2D6, CYP3A4 involved in catalysis of phase I metabolism reactions .Table 9 demonstrates that all compounds were shows inhibitors of five enzymes with probability score ranging from 0.061-0.968.

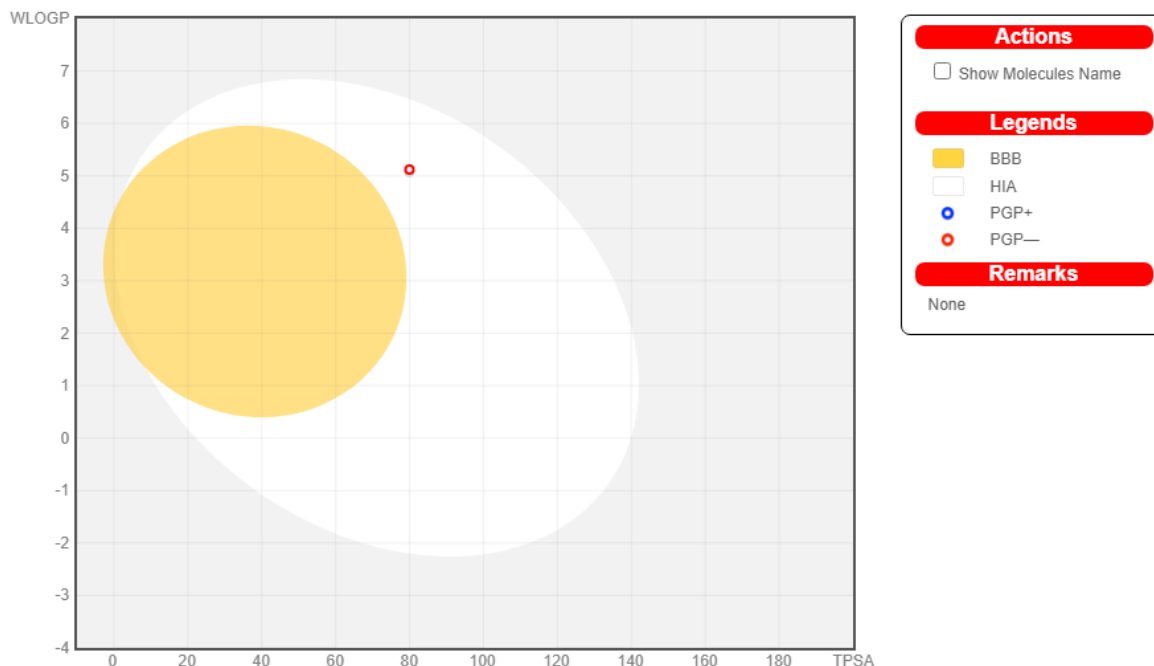


Fig.12.Swiss ADME - bioavailability BOILED-Egg models of 2-[[2-nitro-4-(trifluoromethyl) phenyl]methylidene)-1H-indene-1,3(2H)-dione(Compound 11)

Abbreviation: BBB: blood–brain barrier; HIA: human intestinal absorption; PGP⁺: P-glycoprotein substrate; PGP⁻: P-glycoprotein non-substrate.

Compounds permeability in brain or intestine were estimated using boiled-egg bioavailability model developed using Swiss ADME server based on lipophilicity and polarity indexes. The white sections in egg or yolk indicating coloured spot of physiochemical properties that these compounds are most probably absorbed in GI tract. 2-{{2-nitro-4-(trifluoromethyl) phenyl}methylidene}-1H-indene-1,3(2H)-dione(Compound 11) has good bioavailability lying on top of boiled-egg diagram, as seen in figure 12.

All compounds were estimated to have low clearance rate ranges from 1.057-3.945 mL min⁻¹ kg with exception of compound 8,5,10 which has excretion rate 5.125, 5.32, 5.411 mL min⁻¹ kg respectively with a short half-life of 0.03-0.679 in human body.

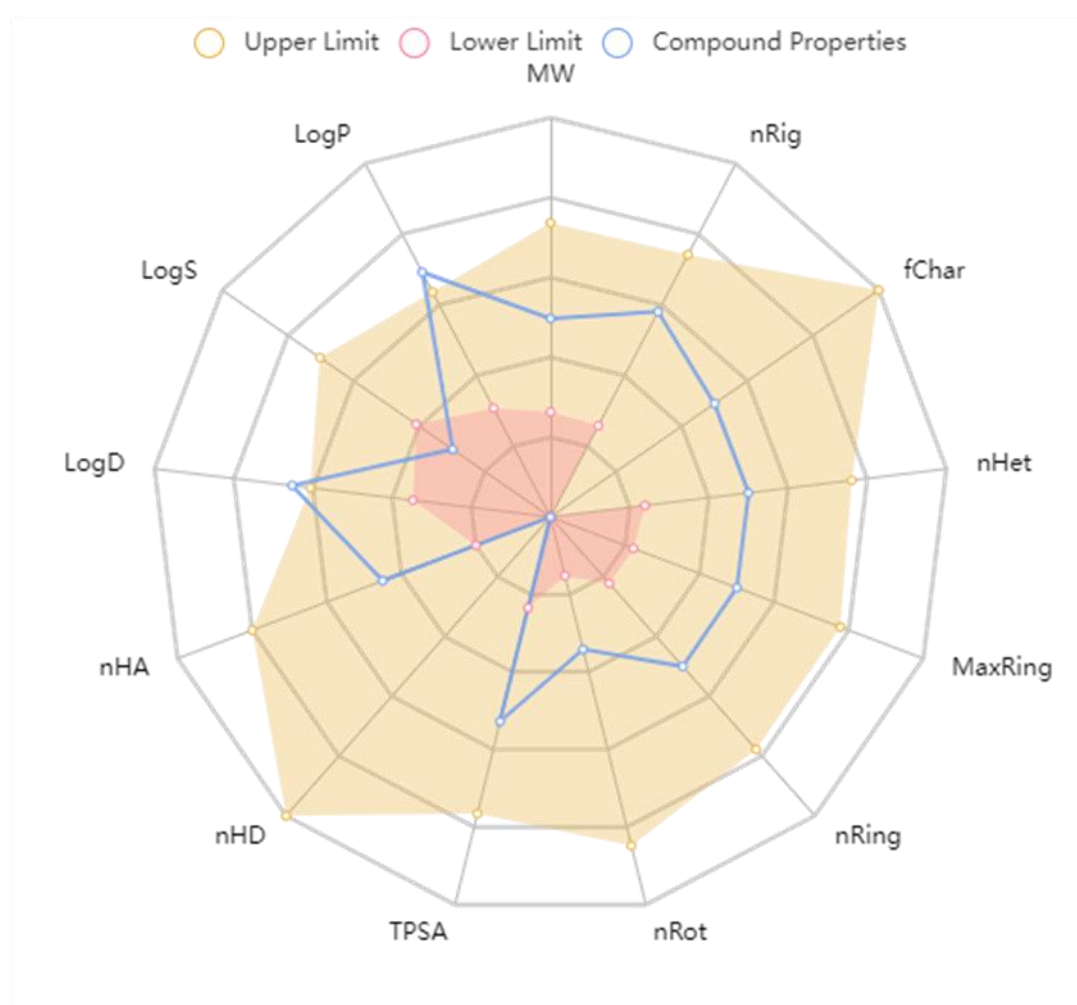


Fig.13 Radar diagram illustrating the physicochemical characteristics of 2-{{2-nitro-4-(trifluoromethyl) phenyl}methylidene}-1H-indene-1,3(2H)-dione(Compound 11).

MW: molecular weight, nRig: number of rigid bonds, fChar: formal charge, nHet: number of heteroatoms, MaxRing: number of atoms in the biggest ring, nRing: number of rings, nRot: number of rotatable bonds, TPSA: topological polar surface area (Å²), nHD: number of hydrogen bond donors, nHA: number of hydrogen bond acceptors, logD: log of octanol partition coefficient at physiological pH 7.4, logS: log of aqueous solubility (mol L⁻¹), and logP: log of octanol partition coefficient

Co m p. No	M W (g/ m ol)	n H A	n H D	T P S A (Å ²)	Con sens us Log Po/ w*	M R	GI Abso rptio n	BB B Per meant	P- gp Sub strate	Lip ins ki	Pfizer	PA IN S (al ert)	Bioav ailabil ity Score	Synt hetic acces sibili ty score
1	28 6.0 2	2	0	34 .1 4	3.81 9	49 .9 1	High	Yes	0	Acc epte d	Rej ecte d	1	0.55	2.064
2	32 9.9 7	2	0	34 .1 4	3.72	74 .4 9	High	Yes	0	Acc epte d	Rej ecte d	1	0.55	2.132
3	29 3.0 7	5	0	77 .2 8	3.11 4	78 .3 4	High	No	0	Acc epte d	Acc epte d	1	0.55	2.271
4	26 8.0 3	2	0	34 .1 4	3.60 5	74 .5 3	High	Yes	0	Acc epte d	Rej ecte d	1	0.55	1.915
5	29 4.0 9	4	0	52 .6	2.89 1	82 .5 1	High	Yes	0.00 1	Acc epte d	Acc epte d	1	0.55	2.075
6	29 0.1 3	2	0	34 .1 4	4.58 3	88 .7 9	High	Yes	0.00 2	Acc epte d	Rej ecte d	1	0.55	1.991
7	23 4.0 7	2	0	34 .1 4	2.92 6	69 .5 2	High	Yes	0	Acc epte d	Acc epte d	1	0.55	1.775
8	28 0.0 7	4	1	63 .6	2.63 4	75 .9 7	High	Yes	0.00 1	Acc epte d	Acc epte d	1	0.55	2.038
9	26 8.0 5	3	1	54 .3 7	3.21 4	78 .0 4	High	Yes	0	Acc epte d	Rej ecte d	1	0.55	2.146
10	25 0.0 6	3	1	54 .3 7	2.70 7	80 .8 2	High	Yes	0	Acc epte d	Acc epte d	1	0.55	1.994
11	34 7.0 4	5	0	77 .2 8	3.50 6	79 .5 4	High	Yes	0	Acc epte d	Acc epte d	1	0.55	2.31
12	27 8.0 9	3	0	43 .3 7	3.41 4	49 .9 1	High	Yes	0	Acc epte d	Rej ecte d	1	0.55	1.875
13	30 1.9 9	2	0	34 .1 4	4.13 8	74 .4 9	High	Yes	0	Acc epte d	Rej ecte d	1	0.55	1.97
14	30 1.9 9	2	0	34 .1 4	4.13 8	78 .3 4	High	No	0	Acc epte d	Rej ecte d	1	0.55	1.97
15	29	4	0	60	3.01	74	High	Yes	0	Acc	Rej	1	0.55	1.903

2.0		.4	1	.5				ep	cte			
7		4		3				d	d			

Table 8. Physicochemical, pharmacokinetics, and medicinal chemistry properties of the compounds 1-15 determined using ADMET 2.0

MW: Molecular Weight; HBA: Num. H-Bond Acceptors; HBD: Num. H-Bond Donors; NRB: Number of rotatable bonds; MR: Molar Refractivity; TPSA: Topological Polar Surface Area; BBB-Blood brain barrier; P-M: Poor-Moderate; P: Poor; GI: Gastrointestinal; P-gp-P Glycoprotein;* Average of five prediction

Metabolism											Elimination	
Com p. No	CYP 1A2-inh	CYP1 A2-sub	CYP 2C19 -inh	CYP 2C19 -sub	CYP 2C9-inh	CYP 2C9-sub	CYP 2D6-inh	CYP 2D6-sub	CYP 3A4-inh	CYP 3A4-sub	CL mL min ⁻¹	T 1/2
1	0.944	0.359	0.92	0.089	0.796	0.789	0.372	0.19	0.115	0.15	2.018	0.053
2	0.953	0.191	0.913	0.09	0.785	0.695	0.268	0.3	0.118	0.139	1.057	0.052
3	0.929	0.425	0.833	0.101	0.868	0.811	0.246	0.421	0.596	0.166	1.707	0.124
4	0.963	0.328	0.899	0.09	0.686	0.362	0.476	0.163	0.126	0.134	2.255	0.144
5	0.952	0.927	0.943	0.463	0.86	0.89	0.214	0.814	0.757	0.269	5.32	0.232
6	0.818	0.613	0.843	0.075	0.734	0.766	0.353	0.182	0.313	0.233	1.567	0.053
7	0.968	0.198	0.833	0.095	0.722	0.493	0.143	0.147	0.061	0.145	2.332	0.023
8	0.939	0.846	0.786	0.07	0.776	0.794	0.412	0.514	0.696	0.18	5.125	0.079
9	0.953	0.186	0.863	0.065	0.747	0.798	0.563	0.382	0.37	0.145	3.945	0.01

												57
10	0.97 2	0.141	0.846	0.063	0.69 9	0.81 9	0.64 2	0.43 2	0.67 5	0.13 5	5.4 11	0.6 4 6
11	0.91 3	0.39	0.908	0.075	0.90 2	0.84	0.22 8	0.27 1	0.55 1	0.11 9	1.7 54	0.0 3
12	0.80 4	0.2	0.702	0.081	0.69 3	0.79 7	0.07 6	0.51 6	0.23	0.17 4	2.3 48	0.1 0 9
13	0.95 4	0.216	0.884	0.071	0.66 8	0.47 2	0.44 9	0.22 8	0.26 6	0.16 5	2.3 12	0.0 7 4
14	0.95 4	0.216	0.884	0.071	0.66 8	0.47 2	0.44 9	0.22 8	0.26 6	0.16 5	2.3 12	0.0 7 4
15	0.89	0.339	0.7	0.068	0.69 2	0.49 7	0.08 8	0.15 4	0.26 6	0.14 3	3.6 94	0.3 5 6
Absorption and Distribution												
Com p. No	Caco-2	MDC K	Pgp-inh	Pgp-sub	HIA	PPB %	VDs	(BB B) penet ratio n (c.br ain/ c.blo od)	Log S			
1	- 4.89 5	9.65E -06	0.987	0	0.00 2	100. 81	0.59 1	0.03 4	- 5.71 6			
2	- 4.87 4	1.17E -05	0.997	0	0.00 4	1.00 4203	0.66 5	0.07 4	- 5.82 2			
3	- 4.80	4.80E -05	0.461	0	0.00 4	1.00 0721	0.56 5	0.09 8	-5.28			

	4											
4	- 4.82 6	9.76E -06	0.977	0	0.00 4	1.00 52	0.65 9	0.04 2	- 5.31 2			
5	- 4.93 3	1.45E -05	0.993	0.001	0.00 4	0.98 8196	0.47 6	0.12 6	- 5.18 6			
6	- 4.99 7	1.10E -05	0.993	0.002	0.00 3	1.00 1129	0.68 8	0.02 2	- 6.14 9			
7	- 4.70 9	1.25E -05	0.93	0	0.00 5	0.99 2157	0.66 3	0.10 2	- 4.75 5			
8	- 4.93 4	1.37E -05	0.5	0.001	0.00 7	0.99 3818	0.45 6	0.26 2	- 4.41 8			
9	- 4.92 4	1.26E -05	0.614	0	0.00 5	1.00 0355	0.58 2	0.21 7	- 4.58 2			
10	- 4.90 1	1.27E -05	0.041	0	0.00 8	0.99 124	0.63	0.25 3	- 4.17 7			
11	- 4.89 2	2.78E -05	0.789	0	0.00 4	1.00 6646	0.55 4	0.09 8	- 5.71 7			
12	- 4.78 3	1.46E -05	0.975	0	0.00 3	0.99 9296	0.66 3	0.03 9	- 5.29 7			
13	- 4.90 3	9.20E -06	0.937	0	0.00 3	1.01 1214	0.57 2	0.02 7	- 5.86 8			
14	- 4.90 3	9.20E -06	0.937	0	0.00 3	1.01 1214	0.57 2	0.02 7	- 5.86 8			
15	- 4.72 2	1.80E -05	0.989	0	0.00 6	1.00 2067	0.64 8	0.04 6	- 4.89 8			
Toxi city												
Com p. No	Ame s	Carci nogen icity	EC (--)	EI (++)	hER G	H- HT	LD ₅₀	Resp irator y toxic ity				
1	++0. 9	++0.8 89	0.003	0.937	--- 0.04 3	++0. 862	0	-- 0.15 6				
2	++0. 873	++0.8 94	0.004	0.967	--- 0.04 6	++0. 823	0	-- 0.15 6				

3	+++ 0.98 1	++0.9 13	0.004	0.984	--- 0.06 3	++0. 814	0	0.46 5				
4	++0. 896	++0.7 93	0.003	0.951	--- 0.06 8	++0. 802	0	-- 0.16 6				
5	++0. 881	++0.9 31	0.004	0.964	--- 0.05 6	-- 0.38 2	0	- 0.51 3				
6	- 0.57 5	++0.7 8	0.003	0.964	--- 0.04 5	+0.5 94	0	-- 0.12 7				
7	+++ 0.91 1	++0.8 09	0.004	0.977	--- 0.03 2	++0. 76	0	-- 0.22 1				
8	+++ 0.91 9	++0.9 18	0.003	0.91	--- 0.05 2	+0.5 15	0	0.29				
9	+++ 0.90 9	++0.9 15	0.004	0.945	--- 0.03 4	++0. 848	0	-- 0.13 3				
10	+++ 0.90 7	++0.8 43	0.004	0.969	--- 0.04 3	+0.5 86	0	-- 0.19 5				
11	+++ 0.96 7	++0.8 32	0.004	0.909	--- 0.15 5	++0. 847	0	++0. 786				
12	+++ 0.92 5	++0.8 90	0.003	0.935	0.13 8	+0.5 98	0	--- 0.07 8				
13	+++ 0.90 4	++0.8 05	0.003	0.923	--- 0.09 2	+0.6 71	0	-- 0.19 5				
14	+++ 0.90 4	++0.8 05	0.003	0.923	--- 0.09 2	+0.6 71	0	--- 0.19 5				
15	+++ 0.92 4	++0.8 40	0.003	0.867	-- 0.16 4	+0.6 05	0	--- 0.07 9				

Table 9. ADMET data of compounds 1-15. The prediction probability values categorized into six symbols represented as endpoints: 0–0.1(---), 0.1–0.3(--), 0.3–0.5(-), 0.5–0.7(+), 0.7–0.9(++), and 0.9–1.0(+++).

2. Conclusion

Novel series of 1, 3-indanedione derivatives were synthesized by using a new procedure with an efficient catalyst and evaluated for their pharmacological potentials regarding antitubercular activities with remarkable yields. Compounds with phenolic group as the terminal substitution or Meta and Para- substitutions are showing moderate to minimum activities, among them electronegative groups like halogens on the aromatic head, were

observed to have higher antitubercular activities. Validation of chemical moieties was done using spectroscopic data and physicochemical property evaluation study. Antitubercular potential of synthesized analogus was investigated by in-vitro screening with standard procedures and found MIC values ranging from 4.5 μ M to 167 μ M. Compounds 1, 10,11,12,15 demonstrated good to exceptional anti-TB efficacy against the Mtb H37Rv strain.

The docked ligands against the protein 6SQ5 vary a binding affinity from -8.8 to -9.9 Kcal/mol, compound 11 shows a greater binding affinity of -9.9 Kcal/mol among all other also compounds. The antitubercular study reveals that among the compounds 1-15 tested, Compound 1, 10, 11, 12, 15 reported with superior antitubercular activity whereas compound numbers 2,3,4,5,6,7,8 and 14 showed moderate activity and 7, 8 showed less activity as compared to standard. The compounds 1, 10, 11, 12 and 15 can be taken as lead molecules where they can be further modified and developed to achieve the good activity.

The in-silico results demonstrate that all of the compounds had a high likelihood of possessing drug-like qualities. Eventually, using SwissADME and ADMETlab2.0 platforms, the in silico ADMET properties study of the final Indane -1, 3(2H)-Dione (1-15) were further assessed for their ADMET and physicochemical characteristics.

The study demonstrated, through various in silico prediction methods that 2-[[2-nitro-4-(trifluoromethyl) phenyl]methylidene]-1H-indene-1,3(2H)-dione, compound 11 exhibits favorable drug-like characteristics, devoid of carcinogenicity and mutagenicity. Molecular docking studies against M. tuberculosis (InhA) with PDB code 6SQ5 provided deeper understanding of designed ligand conformations in the target receptor environment.

Acknowledgement: Authors are thankful for the writing and editing support provided by scientific communications team.

Conflict of Interest: Authors declare no conflicts of interest.

3. References

1. B.S. Furniss, A.J. Hannaford, P.W.G. Smith, A.R. Tatchell, UK, 2004, 5, 1087.
2. Pigot, C., Brunel, D., & Dumur, F. (2022). Indane-1, 3-Dione: From synthetic strategies to applications. *Molecules* (Basel, Switzerland), 27(18), 5976. <https://doi.org/10.3390/molecules27185976>.
3. Giles, D., Prakash, M. S., & Ramseshu, K. V. (2007). Synthesis and biological evaluation of substituted thiophenyl derivatives of indane-1, 3-Dione. *E-Journal of Chemistry*, 4(3), 428–433. <https://doi.org/10.1155/2007/865470>.
4. Jeyachandran, M., & Ramesh, P. (2011). Synthesis, Antimicrobial, and Anticoagulant Activities of 2-(Arylsulfonyl) indane-1, 3-diones. *Organic Chemistry International*, 2011, 1–5. <https://doi.org/10.1155/2011/360810>
5. Giles, D., Roopa, K., Sheeba, F. R., Gurubasavarajaswamy, P. M., Divakar, G., & Vidhya, T. (2012). Synthesis pharmacological evaluation and docking studies of pyrimidine derivatives. *European Journal of Medicinal Chemistry*, 58, 478–484. <https://doi.org/10.1016/j.ejmech.2012.09.050>.
6. R V, Satyendra & Vishnumurthy, K. & Vagdevi, H. & Bhadrappura Lakkappa, Dhananjaya & Shruthi, A. (2015). Synthesis, in vitro anthelmintic, and molecular docking studies of novel 5-nitro benzoxazole derivatives. *Medicinal Chemistry Research*. 24. 10.1007/s00044-014-1207-6.
7. K. Mitka, P. Kowalski, D. Pawelec, Z. Majka, *Croat. Chem. Acta.*, (2009). Synthesis of Novel Indane-1, 3-dione Derivatives and Their Biological Evaluation as Anticoagulant Agents. *Croatica Chemica Acta*, 82. <https://doi.org/10.1039/d3ra00106g>.

8. Sondhi, Sham M., Dinodia, M., Rani, R., Shukla, R., & Raghubir, R. (2009). ChemInform Abstract: Synthesis, antiinflammatory and analgesic activity evaluation of some pyrimidine derivatives. *ChemInform*, 40(24). <https://doi.org/10.1002/chin.200924161>.
9. Varache-Béranger, M., Nuhrich, A., Amiell, J., Dufour, P., & Devaux, G. (1991). Synthèse ET activité anti-inflammatoire de (3, 5-di-tert-butyl-4-hydroxybenzylidène) cyclanones ET composés apparentés. *European journal of medicinal chemistry*, 26(5), 551–556. [https://doi.org/10.1016/0223-5234\(91\)90152-d](https://doi.org/10.1016/0223-5234(91)90152-d).
10. Al-Qaisi, J. A., Alhussainy, T. M., Qinna, N. A., Matalka, K. Z., Al-Kaissi, E. N., & Muhi-Eldeen, Z. A. (2014). Synthesis and pharmacological evaluation of aminoacetylenic isoindoline-1, 3-dione derivatives as anti-inflammatory agents. *Arabian Journal of Chemistry*, 7(6), 1024–1030. <https://doi.org/10.1016/j.arabjc.2010.12.030>.
11. Hadfield, J. A., Pavlidis, V. H., Perry, P. J., & McGown, A. T. (1999). Synthesis and anticancer activities of 4-oxobenzopyrano [2, 3-d]pyrimidines. *Anti-Cancer Drugs*, 10(6), 591–596. <https://doi.org/10.1097/00001813-199907000-00011>.
12. Kim, D. C., Lee, Y. R., Yang, B.-S., Shin, K. J., Kim, D. J., Chung, B. Y., & Yoo, K. H. (2003). Synthesis and biological evaluations of pyrazolo[3,4-d]pyrimidines as cyclin-dependent kinase 2 inhibitors. *European Journal of Medicinal Chemistry*, 38(5), 525–532. [https://doi.org/10.1016/s0223-5234\(03\)00065-5](https://doi.org/10.1016/s0223-5234(03)00065-5).
13. Sondhi, S. M., Goyal, R. N., Lahoti, A. M., Singh, N., Shukla, R., & Raghubir, R. (2005). Synthesis and biological evaluation of 2-thiopyrimidine derivatives. *Bioorganic & Medicinal Chemistry*, 13(9), 3185–3195. <https://doi.org/10.1016/j.bmc.2005.02.047>.
14. Deshmukh, M. B., Salunkhe, S. M., Patil, D. R., & Anbhule, P. V. (2009). A novel and efficient one step synthesis of 2-amino-5-cyano-6-hydroxy-4-aryl pyrimidines and their anti-bacterial activity. *European Journal of Medicinal Chemistry*, 44(6), 2651–2654. <https://doi.org/10.1016/j.ejmech.2008.10.018>.
15. Khairiah Nasser AL-Shammri, Nadia A.A. Elkanzi, Wael A.A. Arafa, Ibrahim O. Althobaiti, Rania B. Bakr, Shaima Mohamed Nabil Moustafa, Novel indan-1,3-dione derivatives: Design, green synthesis, effect against tomato damping-off disease caused by *Fusarium oxysporum* and in silico molecular docking study, *Arabian Journal of Chemistry*, Volume 15, Issue 5, 2022, 103731, <https://doi.org/10.1016/j.arabjc.2022.103731>.
16. H.R. Howard, T.F. Seeger, a Reitz, A. B., & Scott, M. K. (1995). Novel antipsychotics with unique D2/5-HT1A affinity and minimal extrapyramidal side effect liability. In *Advances in Medicinal Chemistry* (pp. 1–55). Elsevier. nnu. Rep. Med. Chem., 1993, 28, 39. [https://doi.org/10.1016/S1067-5698\(06\)80003-9](https://doi.org/10.1016/S1067-5698(06)80003-9).
17. Mishra, Chandra Bhushan, Manral, A., Kumari, S., Saini, V., & Tiwari, M. (2016). Design, synthesis and evaluation of novel indandione derivatives as multifunctional agents with cholinesterase inhibition, anti- β -amyloid aggregation, antioxidant and neuroprotection properties against Alzheimer's disease. *Bioorganic & Medicinal Chemistry*, 24(16), 3829–3841. doi:10.1016/j.bmc.2016.06.027.
18. Thomson, C. G., Duncan, K., Fletcher, S. R., Huscroft, I. T., Pillai, G., Raubo, P., Smith, A. J., & Stead, D. (2006). Sarcosine based indandione hGlyT1 inhibitors. *Bioorganic & Medicinal Chemistry Letters*, 16(5), 1388–1391. <https://doi.org/10.1016/j.bmcl.2005.11.041>.
19. Köhler, F., Fickentscher, K., Halfmann, U. & Koch, H. (1975). Embryotoxicität und Teratogenität von Derivaten des 1, 3-Indandion. *Arch Toxicol* 33, 191–197 (1975). <https://doi.org/10.1007/BF00311272>

20. Buckle, D. R., Morgan, N. J., Ross, J. W., Smith, H., & Spicer, B. A. (1973). Anti-allergic activity of 2-nitroindan 1, 3-diones. *J Med Chem*, 16(12), 1334–1339. doi: 10.1021/jm00270a005.
21. Pluskota, R., Jaroch, K., Kośliński, P., Ziolkowska, B., Lewińska, A., Kruszewski, S., Bojko, B., & Koba, M. (2021). Selected Drug-Likeness Properties of 2-Arylideneindan-1,3-dione Derivatives—Chemical Compounds with Potential Anti-Cancer Activity. *Molecules* (Basel, Switzerland), 26(17), 5256. <https://doi.org/10.3390/molecules26175256>.
22. Meena, Jubie, Pramila, N., M. T., & Gigi. (2023). Synthesis and screening of cyclic diketone indanedione derivatives as future scaffolds for neutrophil elastase inhibition. *RSC Advances*, 13(17), 11838–11852. <https://doi.org/10.1039/d3ra00106g>.
23. Patil, S. A., Patil, R., & Patil, S. A. (2017). Recent developments in biological activities of indanones. *European Journal of Medicinal Chemistry*, 138, 182–198. <https://doi.org/10.1016/j.ejmech.2017.06.032>.
24. Turek, M., Szczęśna, D., Koprowski, M., & Bałczewski, P. (2017). Synthesis of 1-indanones with a broad range of biological activity. *Beilstein Journal of Organic Chemistry*, 13, 451–494. <https://doi.org/10.3762/bjoc.13.48>.
25. Menezes, J. C. J. M. D. S. (2017). Arylidene indanone scaffold: medicinal chemistry and structure–activity relationship view. *RSC Advances*, 7(15), 9357–9372. <https://doi.org/10.1039/c6ra28613e>.
26. Buckingham, J. *Dictionary of Natural Products, Supplement 1*, 1st ed.; Taylor & Francis: New York, NY, USA, 1994; ISBN 978-1-00-305992-9.
27. Pigot, C., Noirbent, G., Bui, T.-T., Peralta, S., Gimes, D., Nechab, M., & Dumur, F. (2019). Push-pull chromophores based on the naphthalene scaffold: Potential candidates for optoelectronic applications. *Materials*, 12(8), 1342. <https://doi.org/10.3390/ma12081342>.
28. Smith, M. B., & March, J. (2007). *March's advanced organic chemistry: reactions, mechanisms, and structure* (6th Ed.). Wiley, page no-945.
29. R. J. Sundberg, “The Chemistry of Indoles,” Academic Press, New York, 1996.
30. World Health Organization (WHO). *Global Tuberculosis Report* [Internet]. Geneva: WHO; <https://www.who.int/teams/global-tuberculosis-programme/tb-reports/global-tuberculosis-report-2023>.
31. Dheda K, Barry CE 3rd, Maartens G. Tuberculosis. *Lancet*. 2016; 387(10024):1211-1226. Doi: 10.1016/S0140-6736(15)00151-8.
32. Pai M, Behr MA, Dowdy D, et al. Tuberculosis. *Nat Rev Dis Primers*. 2016; 2:16076. doi:10.1038/nrdp.2016.76.
33. Schito M, Peter J, Cavanaugh S, et al. Opportunities and challenges for cost-effective implementation of new point-of-care diagnostics for tuberculosis. *J Infect Dis*. 2021; 222(Suppl 6):S525-S534. doi:10.1093/infdis/jiaa446.
34. Zumla A, Raviglione M, Hafner R, von Reyn CF. Tuberculosis. *N Engl J Med*. 2013; 368(8):745-755. Doi: 10.1056/NEJMra1200894.
35. Khan N, Mendonca L, Dhariwal A, et al. Gut microbiome modulates tuberculosis susceptibility and treatment outcome. *J Exp Med*. 2020; 217(11):e20191181. doi:10.1084/jem.20191181.
36. World Health Organization (WHO). *Global Tuberculosis Programme: Drug-resistant Tuberculosis* [Internet]. Geneva: WHO; [cited 2024 Mar 26]. Available from: <https://www.who.int/teams/global-tuberculosis-programme/drug-resistant-tuberculosis>.
37. Furniss BS, Hannaford AJ, Rogers V, Smith PWG. *Vogel's Textbook of Practical Organic Chemistry*. 4th ed. ELBS Great Britain; 1984. 860 p.
38. Meena, Shamendra & Durairaj, Shankar & Ramseshu, K. & D., Giles & Prakash, M. & Venkataraman, S... (2006). Synthesis of 2-(Arylmethylene)-(1H)-indane-1,3-(2H)-

- diones as Potential Fungicidal and Bactericidal Agents. *Cheminform.* 37. 10.1002/chin.200640094.
39. Rajendran, Karthik & Sajini, Jasmin & Sasikumar, S. & Betanabhatla, K.S. & Christina, A.J.M. & Athimoolam, J. & Saravanan, K.S.. (2008). Evaluation of anti-tubercular activity of some synthesised benz spiro-oxirane derivatives of indane-1, 3-dione. *Pharmacologyonline.* 2. 176-191.
 40. [40] D., Giles & PRAKASH, M. & RAMSESHU, K. (2007). Synthesis and Biological Evaluation of Substituted Thiophenyl Derivatives of Indane-1, 3-Dione. *E-Journal of Chemistry.* 4. 428-433. 10.1155/2007/865470.
 41. Hilgetag G and Martini A, *Preparative organic chemistry*, John Wiley & Sons, New York. 1972. 508-512.
 42. Morris, Garrett M., Huey, R., Lindstrom, W., Sanner, M. F., Belew, R. K., Goodsell, D. S., & Olson, A. J. (2009). AutoDock4 and AutoDockTools4: Automated docking with selective receptor flexibility. *Journal of Computational Chemistry*, 30(16), 2785–2791. doi:10.1002/jcc.21256.
 43. Kitchen DB, Decornez H, Furr JR, Bajorath J. Docking and scoring in virtual screening for drug discovery: methods and applications. *Nat Rev Drug Discov.* 2004; 3 (11):935-949.
 44. Hunter, A. D. (1997). ACD/ChemSketch 1.0 (freeware); ACD/ChemSketch 2.0 and its Tautomers, Dictionary, and 3D Plug-ins; ACD/HNMR 2.0; ACD/CNMR 2.0. *Journal of Chemical Education*, 74(8), 905. Doi: 10.1021/ed074p905.
 45. Pettersen, E. F., Goddard, T. D., Huang, C. C., Couch, G. S., Greenblatt, D. M., Meng, E. C., & Ferrin, T. E. (2004). UCSF Chimera—A visualization system for exploratory research and analysis. *Journal of Computational Chemistry*, 25(13), 1605–1612. doi:10.1002/jcc.20084
 46. Sabbah M, Mendes V, Vistal RG, Dias DMG, Záhorszka M, Mikušová K, Korduláková J, Coyne AG, Blundell TL, Abell C. Fragment-Based Design of Mycobacterium tuberculosis InhA Inhibitors. *J Med Chem.* 2020 May 14; 63(9):4749-4761. doi: 10.1021/acs.jmedchem.0c00007. Epub 2020 Apr 15. Erratum in: *J Med Chem.* 2020 Aug 13;63(15):8650. PMID: 32240584; PMCID: PMC7232676.
 47. Adeniji, Shola Elijah, Sani Uba, and Adamu Uzairu. "Multi-linear regression model, molecular binding interactions and ligand-based design of some prominent compounds against Mycobacterium tuberculosis." *Network Modeling Analysis in Health Informatics and Bioinformatics* 9 (2020): 1-18.
 48. Shola Elijah Adeniji, Sani Uba, Adamu Uzairu, Theoretical modeling and molecular docking simulation for investigating and evaluating some active compounds as potent anti-tubercular agents against MTB CYP121 receptor, *Future Journal of Pharmaceutical Sciences*, Volume 4, Issue 2, 2018, Pages 284-295, <https://doi.org/10.1016/j.fjps.2018.10.003>.
 49. Ibrahim, M. T., Uzairu, A., Shallangwa, G. A., & Uba, S. (2020). In-silico activity prediction and docking studies of some 2, 9-disubstituted 8-phenylthio/phenylsulfinyl-9h-purine derivatives as Anti-proliferative agents. *Heliyon*, 6(1), e03158. doi:10.1016/j.heliyon.2020.e03158
 50. Dallakyan S, Olson AJ. Small-molecule library screening by docking with PyRx. *Methods Mol Biol.* 2015; 1263:243-50. doi: 10.1007/978-1-4939-2269-7_19. PMID: 25618350.
 51. Gaillard, Thomas. (2018). Evaluation of AutoDock and AutoDock Vina on the CASF-2013 benchmark. *Journal of Chemical Information and Modeling*, 58(8), 1697–1706. doi:10.1021/acs.jcim.8b00312.
 52. Siddiqui, F.A., Khan, S.L., Marathe, R.P., Nema, N. V., 2021. Design, Synthesis, and In Silico Studies of Novel N-(2-Aminophenyl)-2,3- Diphenylquinoxaline-6-

- Sulfonamide Derivatives Targeting Receptor- Binding Domain (RBD) of SARS- CoV-2 Spike Glycoprotein and their Evaluation as Antimicrobial and Antimalarial Agents. *Letts. Drug Des. Discov.* 18, 915–931. <https://doi.org/10.2174/1570180818666210427095203>.
53. Prakash Jayavel, Venkateswaramoorthi Ramasamy, Napolraj Amaladoss, Vijayakumar Renganathan, Vasy I Shupeniuk, A facile synthesis, characterization, DFT, ADMET and in-silico molecular docking analysis of novel 4-ethyl acridine-1,3,9 (2,4,10H)-trione, *Chemical Physics Impact*, Volume 8, 2024, 100476, <https://doi.org/10.1016/j.chphi.2024.100476>.
 54. Markus Wiederstein, Manfred J. Sippl, ProSA-web: interactive web service for the recognition of errors in three-dimensional structures of proteins, *Nucleic Acids Research*, Volume 35, Issue suppl_2, 1 July 2007, Pages W407–W410, <https://doi.org/10.1093/nar/gkm290>.
 55. Laskowski, Roman & Macarthur, M.W. & Moss, D.S. & Thornton, Janet. (1993). PROCHECK: A program to check the stereochemical quality of protein structures. *Journal of Applied Crystallography*. 26. 283-291. 10.1107/S0021889892009944.
 56. Maria, C. S. L.; Marcus, V. N.; de Souza. Alessandra, C. P.; Marcelle de, L. F.; Raoni S. B. G.; Thais Cristina, M. N.; Monica, A. P. Evaluation of anti-tubercular activity of nicotinic and isoniazid analogues. *ARKIVOC* 2007, 2007, 181–191.
 57. Karthik, R.; Jasmin Sajni, R.; Sasikumar, S.; Kalyan, S.B.; Christina, A.J.M.; Jagan, A.; Sundara Saravanan, K. Evaluation of Anti-Tubercular Activity of Some Synthesised Benz Spiro-Oxirane Derivatives of Indane-1,3-Dione. *Pharmacologyonline* 2008, 2, 176–191.
 58. Franzblau, Scott G., Witzig, R. S., McLaughlin, J. C., Torres, P., Madico, G., Hernandez, A., ... Gilman, R. H. (1998). Rapid, low-technology MIC determination with clinical Mycobacterium tuberculosis isolates by using the microplate Alamar Blue assay. *Journal of Clinical Microbiology*, 36(2), 362–366. doi:10.1128/jcm.36.2.362-366.1998
 59. Prasad, S. R., Satyanarayan, N. D., Shetty, A. S. K., & Thippeswamy, B. (2022). Synthesis, antimicrobial, and antitubercular evaluation of new Schiff bases with in silico ADMET and molecular docking studies. *European Journal of Chemistry*, 13(1), 109–116. doi:10.5155/eurjchem.13.1.109-116.2216.
 60. Prakash Jayavel, Venkateswaramoorthi Ramasamy, Napolraj Amaladoss, Vijayakumar Renganathan, Vasy I Shupeniuk, A facile synthesis, characterization, DFT, ADMET and in-silico molecular docking analysis of novel 4-ethyl acridine-1,3,9 (2,4,10H)-trione, *Chemical Physics Impact*, Volume 8, 2024, 100476, <https://doi.org/10.1016/j.chphi.2024.100476>.
 61. Lagunin A, Zakharov A, Filimonov D, Poroikov V. QSAR Modelling of Rat Acute Toxicity on the Basis of PASS Prediction. *Mol Inform.* 2011 Mar 14; 30(2-3):241-50. doi: 10.1002/minf.201000151. Epub 2011 Mar 18. PMID: 27466777.
 62. Maunz, A., Gütlein, M., Rautenberg, M., Vorgrimmler, D., Gebele, D., Helma, C., & Lazar. (2013). Lazar: A modular predictive toxicology framework. *Frontiers in Pharmacology*, 4. <https://doi.org/10.3389/fphar.2013.00038>.
 63. Ahmed A, Saeed A, Ejaz SA, Aziz M, Hashmi MZ, Channar PA, Abbas Q, Raza H, Shafiq Z, and El-Seedi HR. Novel adamantyl clubbed iminothiazolidinones as promising elastase inhibitors: design, synthesis, molecular docking, ADMET and DFT studies. *RSC Adv.* 2022 Apr 19; 12(19):11974-11991. doi: 10.1039/d1ra09318e. PMID: 35481107; PMCID: PMC9016748.
 64. Banerjee P, Eckert AO, Schrey AK, Preissner R. ProTox-II: a webserver for the prediction of toxicity of chemicals. *Nucleic Acids Res.* 2018 Jul 2; 46(W1):W257-W263. doi: 10.1093/nar/gky318. PMID: 29718510; PMCID: PMC6031011.

65. Drwal MN, Banerjee P, Dunkel M, Wettig MR, Preissner R. ProTox: a web server for the in silico prediction of rodent oral toxicity. *Nucleic Acids Res.* 2014 Jul; 42(Web Server issue):W53-8. doi: 10.1093/nar/gku401. Epub 2014 May 16. PMID: 24838562; PMCID: PMC4086068.
66. Daina A, Zoete V. A BOILED-Egg to Predict Gastrointestinal Absorption and Brain Penetration of Small Molecules. *ChemMedChem.* 2016 Jun 6; 11(11):1117-21. doi: 10.1002/cmdc.201600182. Epub 2016 May 24. PMID: 27218427; PMCID: PMC5089604.